Supporting Information

Non-transgenic gene modulation *via* spray delivery of nucleic acid/peptide complexes into plant nuclei and chloroplasts

Chonprakun Thagun[1], *Yoko Horii*[2], *Maai Mori*[2], *Seiya Fujita*[1], *Misato Ohtani*[3], *Kousuke Tsuchiya*[1,2], *Yutaka Kodama*[2,4], *Masaki Odahara*[2]* *and Keiji Numata*[1,2]*.

[1] Department of Material Chemistry, Graduate School of Engineering, Kyoto University, Kyoto-Daigaku-Katsura, Nishikyo-ku, Kyoto 615-8510, Japan

[2] Biomacromolecules Research Team, RIKEN Center for Sustainable Resource Science, 2-1 Hirosawa, Wako-shi, Saitama 351-0198, Japan

[3] Department of Integrated Biosciences, Graduate School of Frontier Sciences, The University of Tokyo, 5-1-5 Kashiwanoha, Kashiwa, Chiba, 277-8562, Japan

[4] Center for Bioscience Research and Education, Utsunomiya University, Tochigi 321-8505, Japan.

Figure S1-S26

Table S1-S11

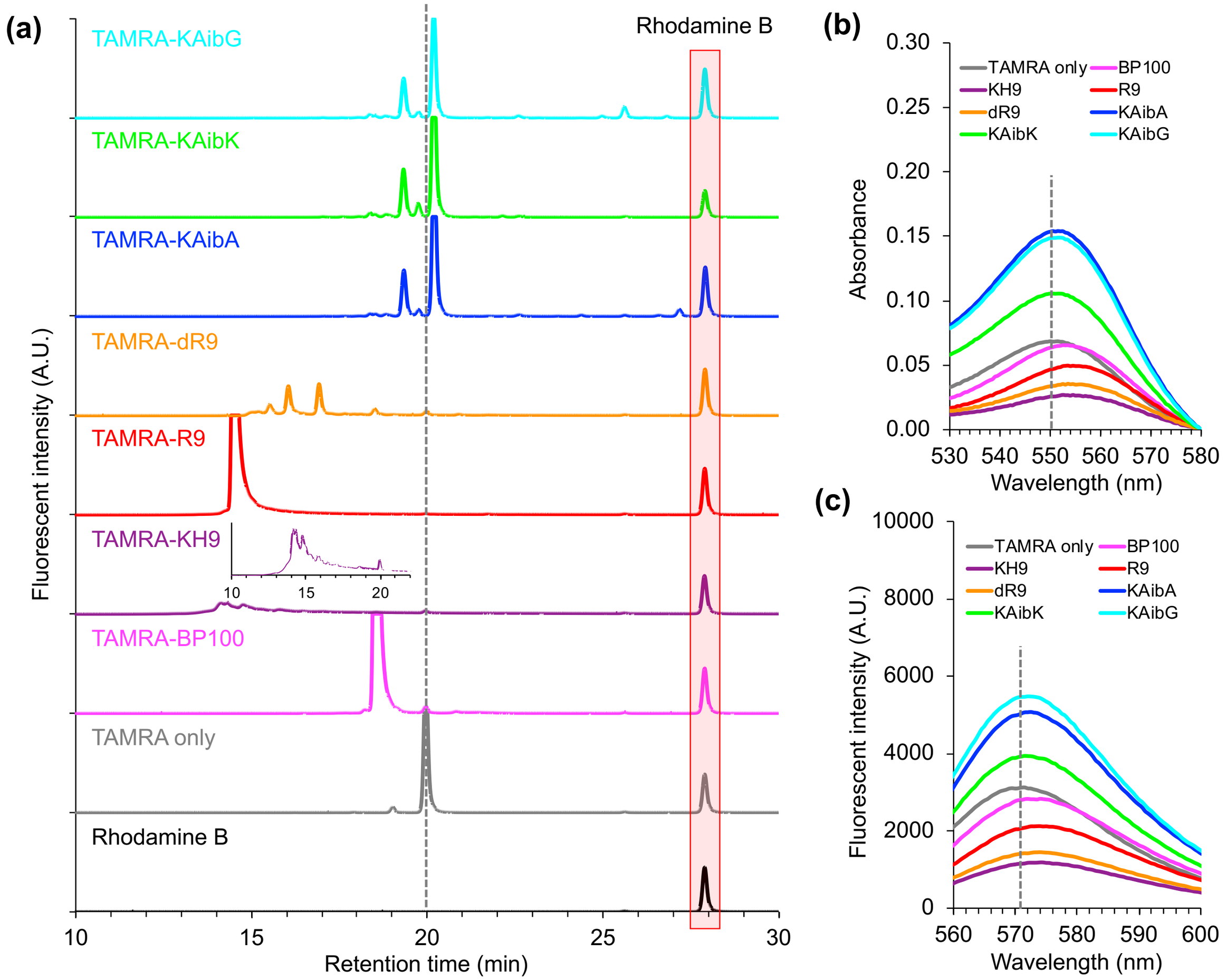

Figure S1. Covalently conjugation of TAMRA fluorescent dye to CPPs.
(a) Fluorescence chromatograms of different TAMRA-CPP conjugates. Solutions containing 0.1 μg of TAMRA-CPPs and free TAMRA fluorescence dye were mixed with 0.05 μg of Rhodamine B (as an internal standard) and analyzed by reverse-phase high-performance liquid chromatography with the fluorescence detection (Ex/Em = 545/575 nm). **(b)** Absorbance spectra of different TAMRA-CPPs in water (0.1 μg /μl) analyzed by UV-Vis spectrophotometry. **(c)** Fluorescence emission spectra of different TAMRA-CPPs solutions (0.1 μg /μl) analyzed by fluorescence spectrometry with excitation wavelength of 550 nm. Dashed lines in **(a)** to **(c)** indicate the peak tops of free TAMRA molecules in the chromatogram and spectra.

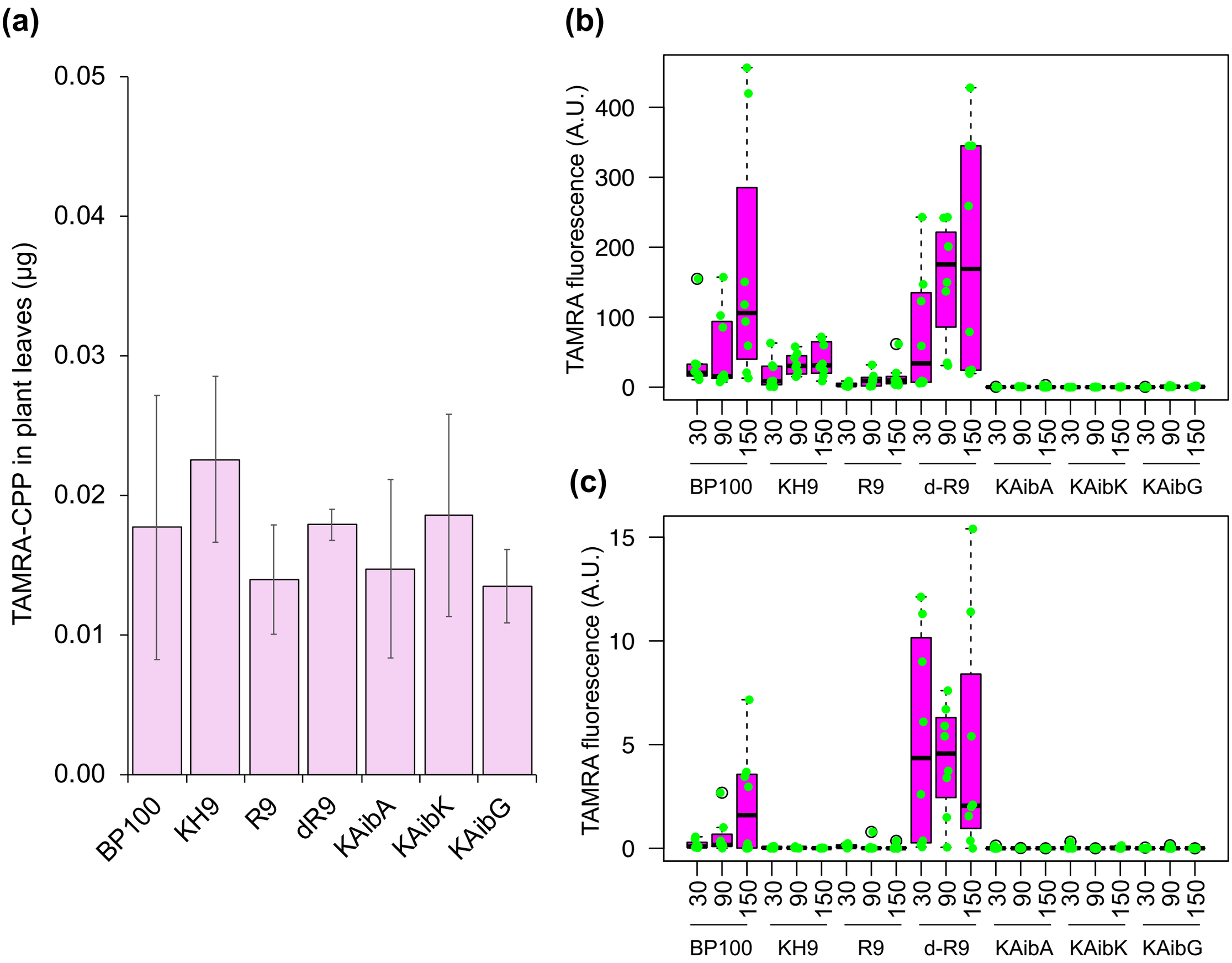

Figure S2. Fluorescent signals of TAMRA-labeled CPPs in Arabidopsis leaves
(a) Amounts of different TAMRA-labeled CPPs reached *Arabidopsis thaliana* (eco. *col-0*) leaves after 30 minutes of spray application. After spraying and incubation, plant leaf lysates were prepared as described in the Methods section. TAMRA fluorescence in lysates was determined by fluorospectrometry with ex/em wavelength of 545/580 nm. Error bar = standard deviation of 4 replicates. **(b)** Fluorescent intensity of TAMRA-labeled CPP in epidermal cells and **(c)** palisade mesophylls of *A. thaliana* leaves at 30, 90, and 150 min post spraying. Fluorescent images were collected from 8 ROIs in biological independent leaves and analyzed by Fiji ImageJ. The distributions of fluorescent intensities of TAMRA-labeled CPPs in plant leaves after spraying were shown as box plot (n = 8). Green dots represent each data point and black bars are the medians of distributed values. Black circles are the outliers.

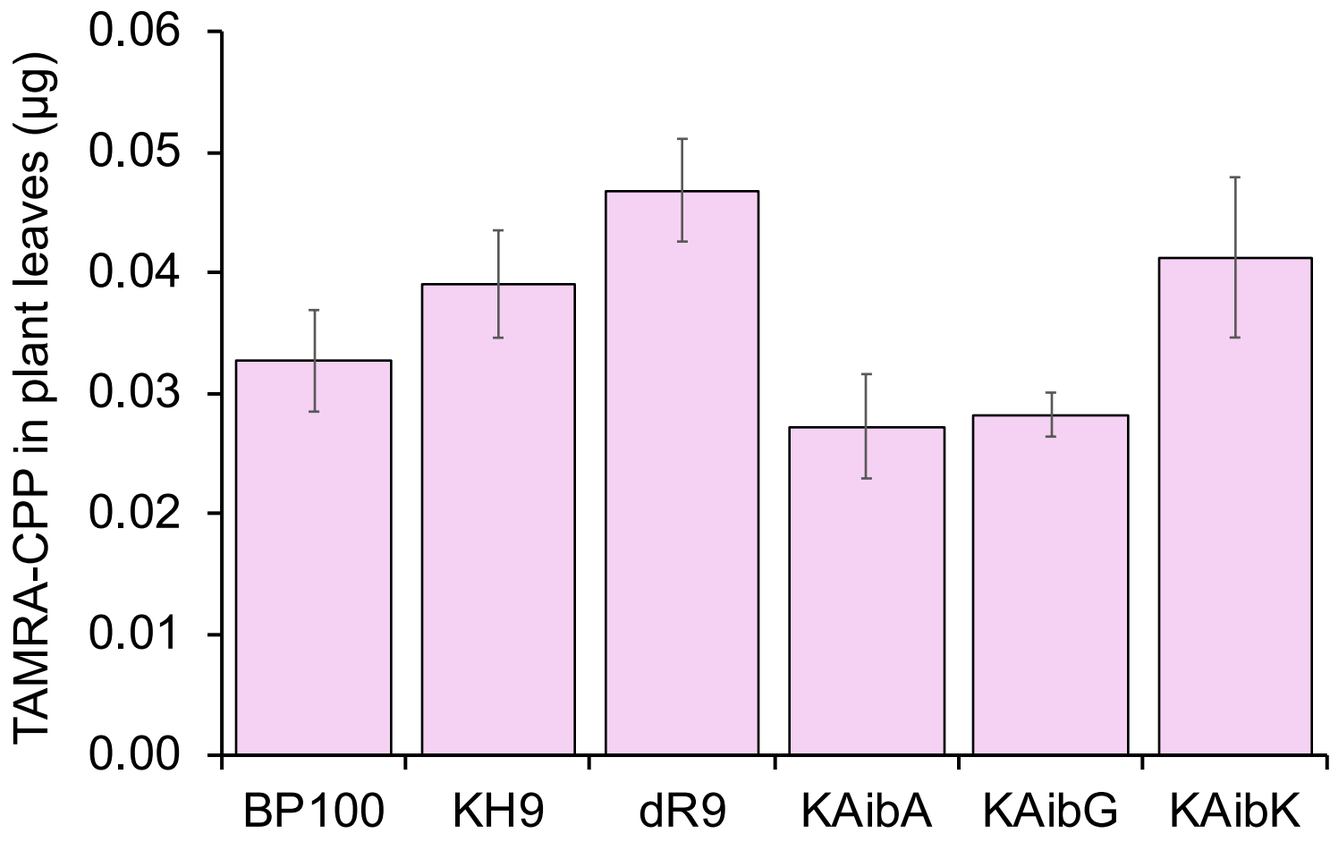

Figure S3. Abundance of different TAMRA-labeled CPPs in soybean leaves after foliar spraying.
Glycine max (cv. Enrei) were sprayed with different solutions containing 0.1 µg of TAMRA-CPPs and incubated for 30 minutes. Leaf lysates were extracted by 1xPBS buffer (pH 7.4) supplemented with 0.1% Triton-X100 and fluorescent intensities of TAMRA in samples were measured using fluorospectrometric analysis. Error bars = standard deviations of the average values of 4 replicates.

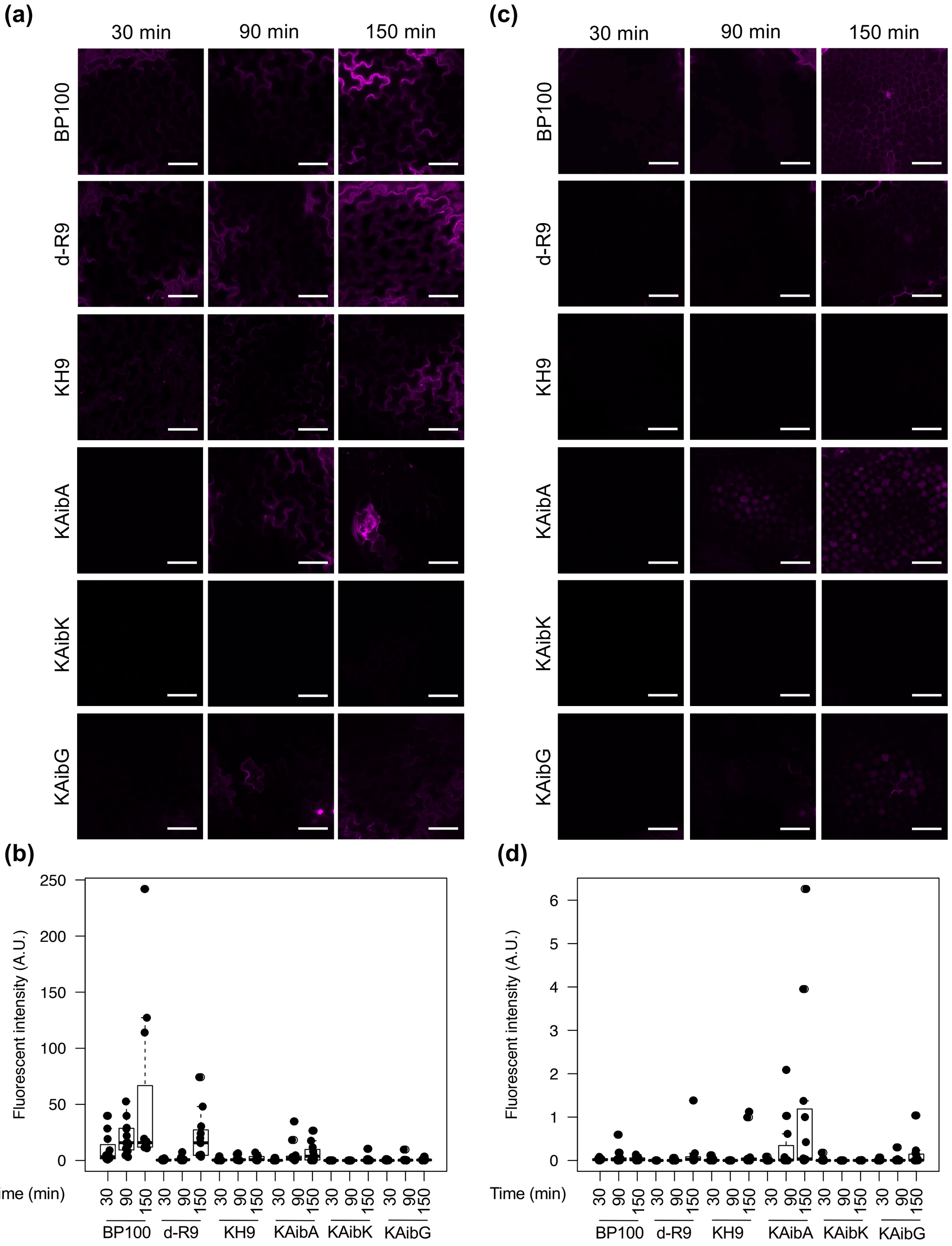

Figure S4. Translocation of TAMRA-labeled CPPs in soybean (*Glycine max* cv. Enrei) leaves **(a)** and **(b)** Fluorescent intensity of TAMRA-labeled CPP in epidermal cells of soybean leaves at 30, 90 and 150 min post spraying. **(c)** and **(d)** Fluorescent intensity of TAMRA-labeled CPPs in palisade mesophyll of soybean leaves. The TAMRA-CPPs spraying experiments on soybean leaves were repeated twice. Fluorescent images of each TAMRA-CPP were taken from 6 ROIs of leaf epidermal cells and palisade mesophyll layer (3 ROIs per leaf) and analyzed by Fiji ImageJ. The distributions of fluorescent intensities of TAMRA-labeled CPPs in plant leaves after spraying were shown as box plot in **(b)** and **(d)**. Dots represent each data point and black bars are the medians of distributed values. Scale bars = 50 μm.

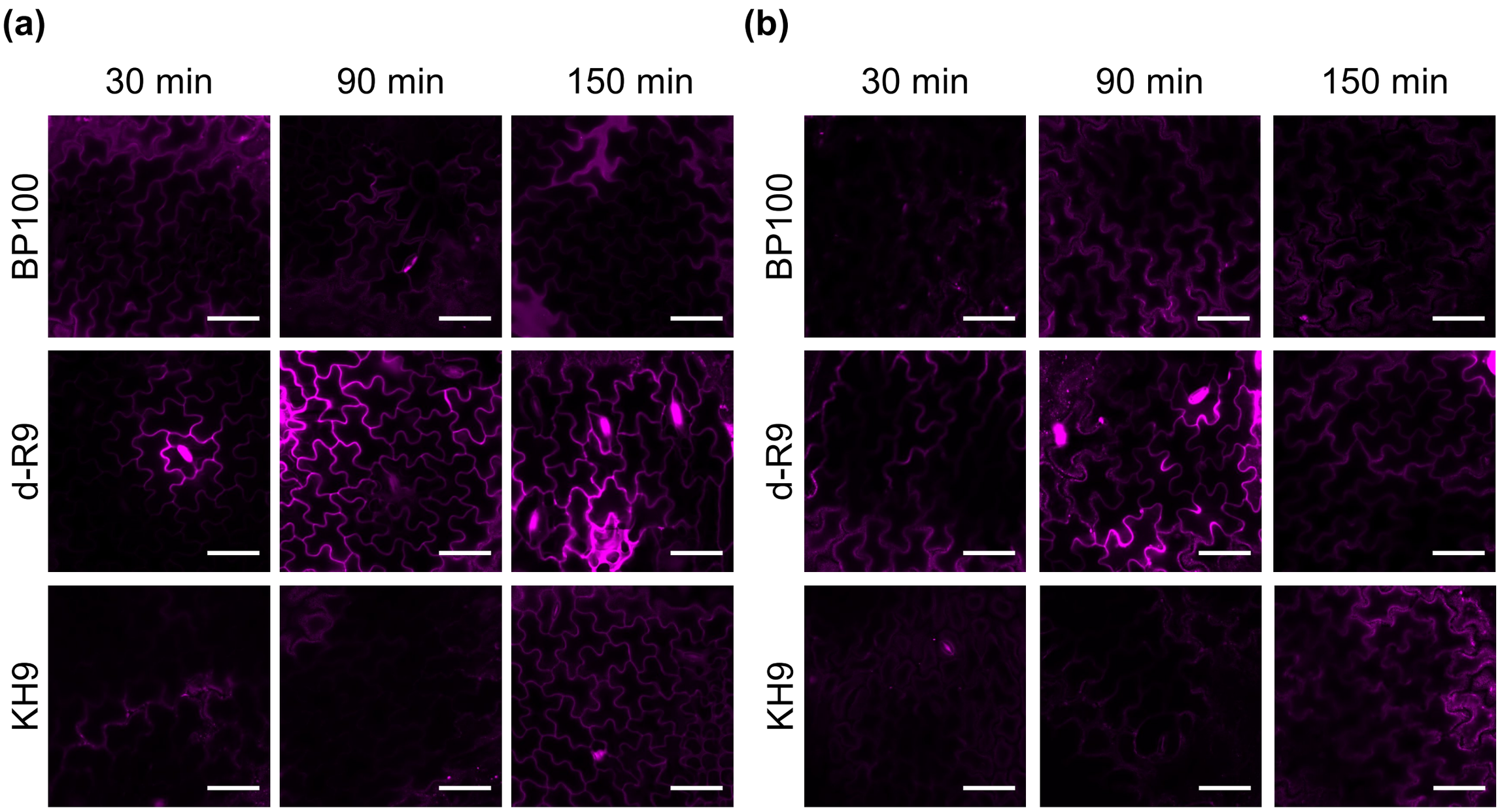

Figure S5. Translocation of TAMRA-labeled CPPs in leaf epidermal cells of two different soybean cultivars
(a) and **(b)** Fluorescent intensity of TAMRA-labeled CPP in epidermal cells of soybean leaves ((**a)** Peking and (**b)** William-82, respectively) at 30, 90 and 150 min post spraying. Scale bars = 50 μm.

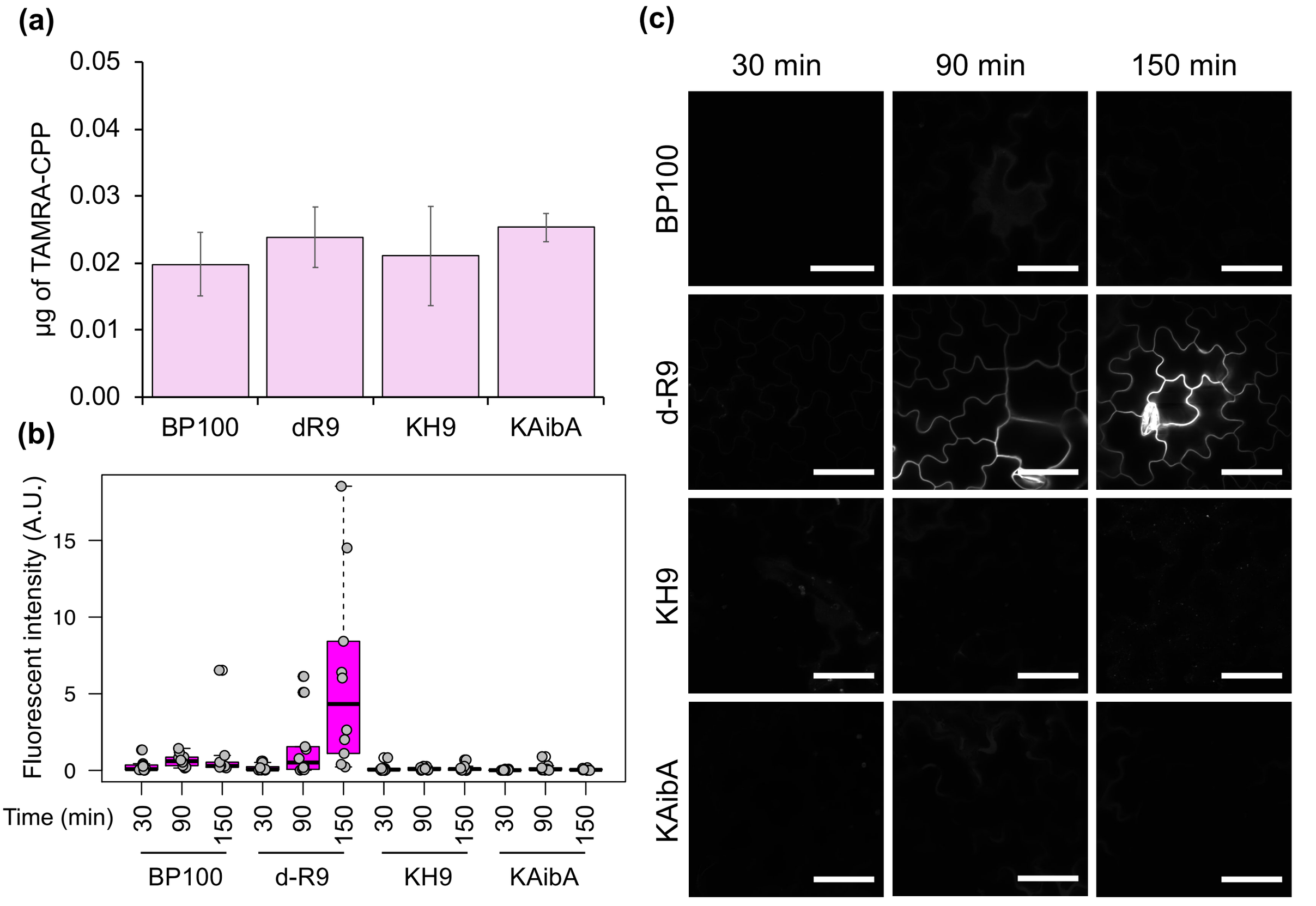

Figure S6. Translocation of TAMRA-labeled CPPs in leaf epidermal cells of tomato
(a) Reaching of spray solutions containing 0.1 µg/ml of different TAMRA-CPP to tomato leaves after foliar application for 30 minutes. Tomato leaf extracts were prepared as described in the Methods section. Fluorescent intensities of TAMRA-labeled CPPs in plant lysates were determined by fluorospectrometry with ex/em = 545/580 nm. Error bars = standard deviations of the average values of 4 replicates. **(b)** and **(c)** Fluorescent intensity of TAMRA-labeled CPP in epidermal cells of tomato leaves at 30, 90, and 150 min post spraying. The spray experiments of TAMRA-CPPs to tomato leaves were repeated twice. The distributions of fluorescent intensities in 10 ROIs collected from two TAMRA-labeled CPPs sprayed leaves (5 ROIs per leaf) were shown as box plot in **(b).** Dots represent each data point and black bars are the medians of distributed values. Scale bars = 50 µm.

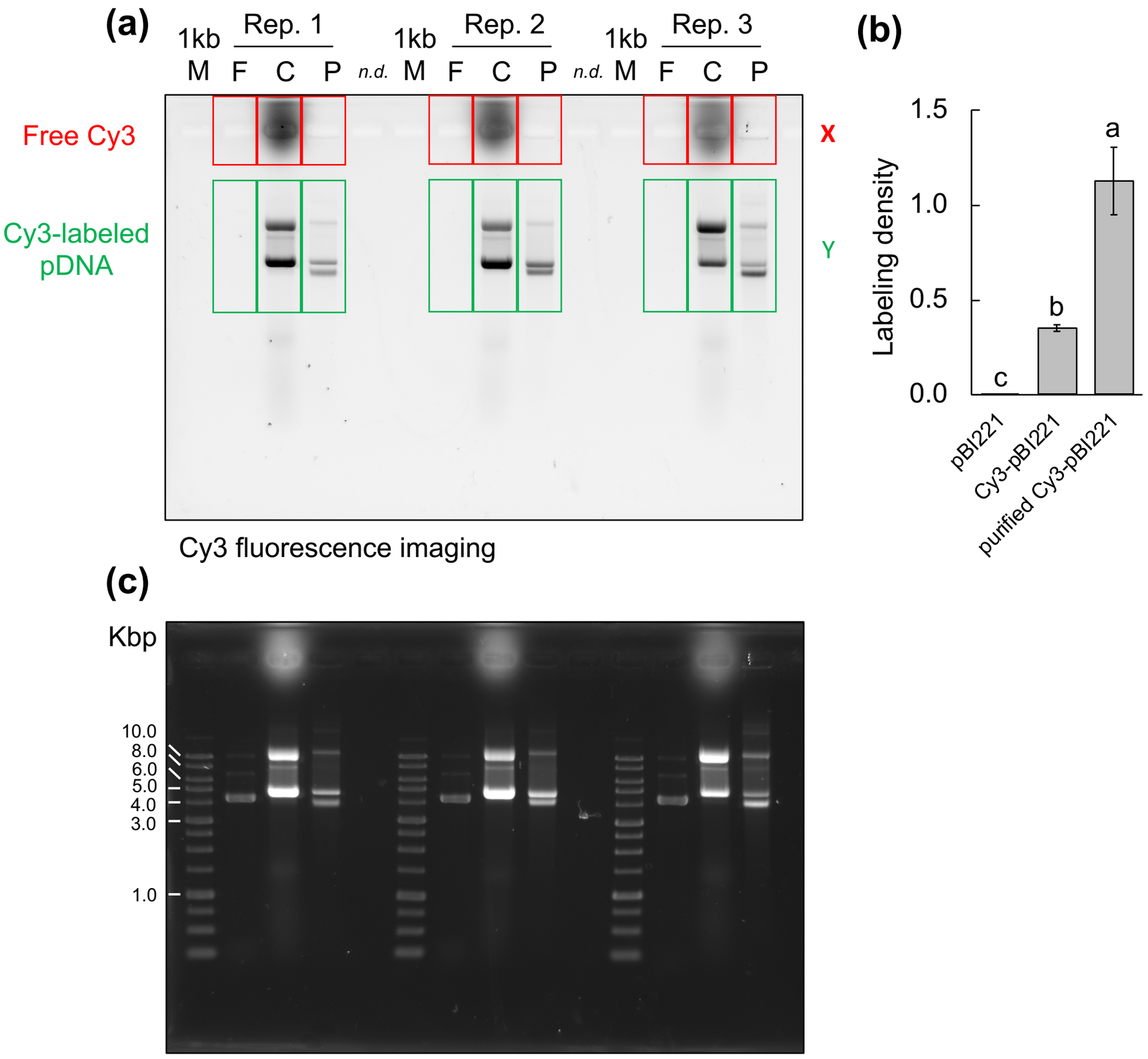

Figure S7. Labeling of pBI221 plasmid DNA with Cy3 fluorescent dye
(a) pBI221 was labeled with Cyanine-3 (Cy3) fluorescent dye and analyzed in 0.8% agarose gel electrophoresis in 1X TAE buffer at 50 volts for 1 hour. Agarose gel was then exposed with LED light with CyanoView filter under CCD camera of LuminoGraphI (ATTO Corporation, Tokyo, Japan) to visualized Cy3-labeled pBI221 molecules and free Cy3 florescent dye. The labeling experiments were replicated 3 times (Rep 1-3). F = Free pBI221, C = Cy3-conjugated pBI221, P = purified Cy3-labeled pBI221, and *n.d.* = empty lanes. The intensities of plasmid DNA bands and free Cy3 molecules in the agarose gel were quantified by Fiji ImageJ. **(b)** Labeling density of Cy3 to pBI221 molecules were calculated regarding the following equation,

$$Labeling\ density = Band\ intensity\ of\ (\frac{Y}{X+Y})$$

Letters indicate statistical differences among samples analyzed by one-way ANOVA with Tukey's HSD test at $p = 0.05$ ($n = 3$). **(c)** An autograph of ethidium bromide-stained agarose gel as in **(a)**. Kbp is kilobase pairs.

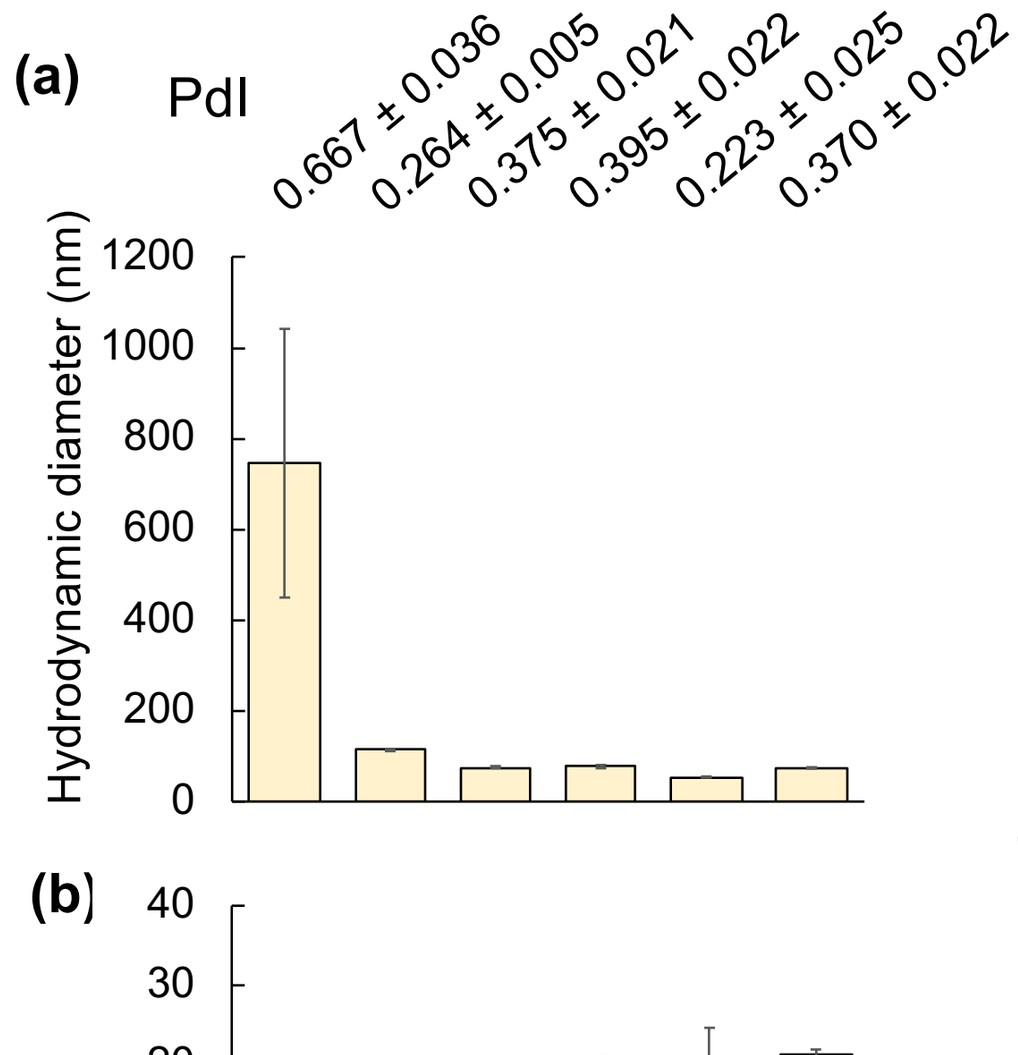

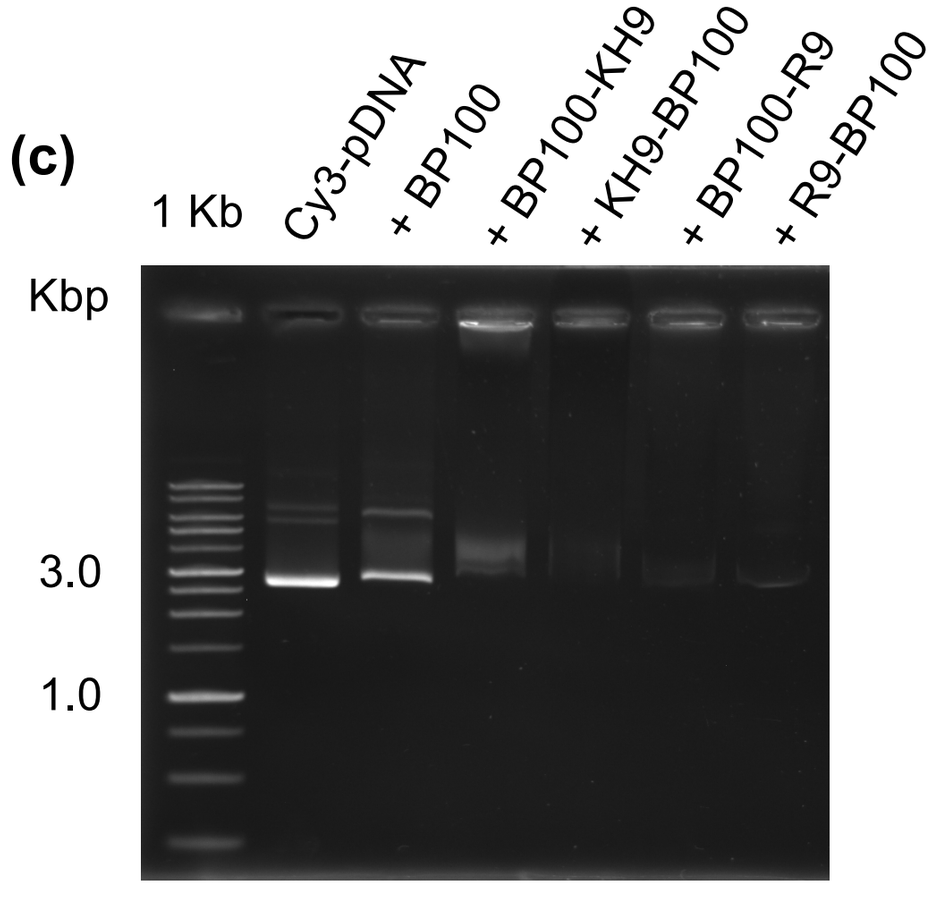

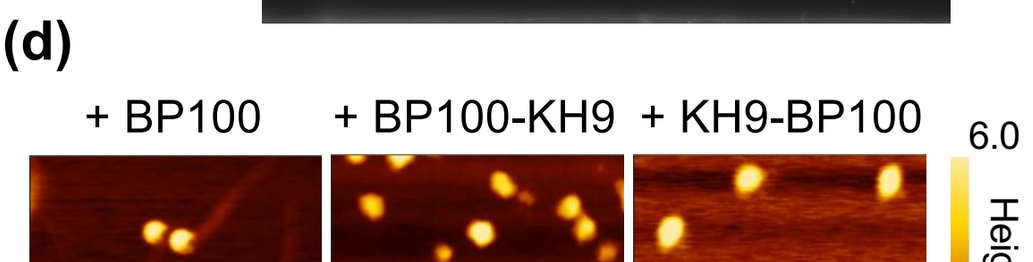

Figure S8. Physicochemical properties of different Cy3-labeled pDNA/CPP complexes formed at N/P ratio = 2.0

(a) Hydrodynamic diameter and **(b)** zeta-potential of different Cy3-labeled pDNA/CPP complexes formed at N/P ratio = 2.0. Error bars = SD of average values (*n* = 5). **(c)** Agarose gel mobility shift assay of different Cy3-labeled pDNA/CPP complexes formed at N/P ratio = 2.0. **(d)** AFM images of complexes between Cy3-labeled pDNA and different cationic CPPs on the mica surface. Heat map represents the height of complexes and scale bars is 200 nm.

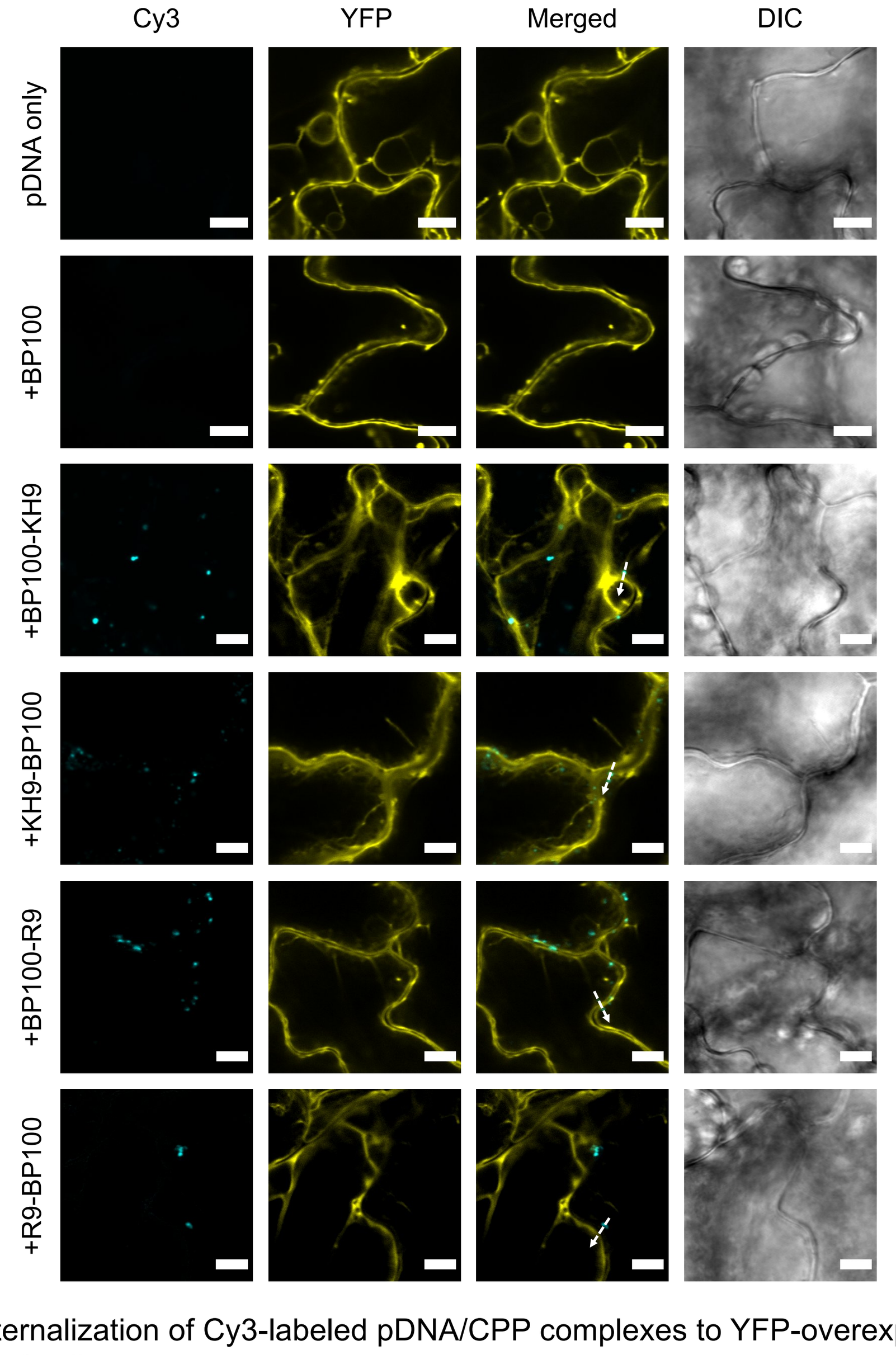

Figure S9. Internalization of Cy3-labeled pDNA/CPP complexes to YFP-overexpressing Arabidopsis leaf cell

Internalization of different Cy3-labeled pDNA/CPP complexes in epidermal cells of transgenic leaves of *Arabidopsis thaliana* overexpressing YFP at 2 hours post spraying. YFP fluorescence was shown as yellow color in this figure. Arrows on top of the selected particles show directions of fluorescent profiles in enlarged images in **Figure 2e** to **h**. Scale bars = 10 μm.

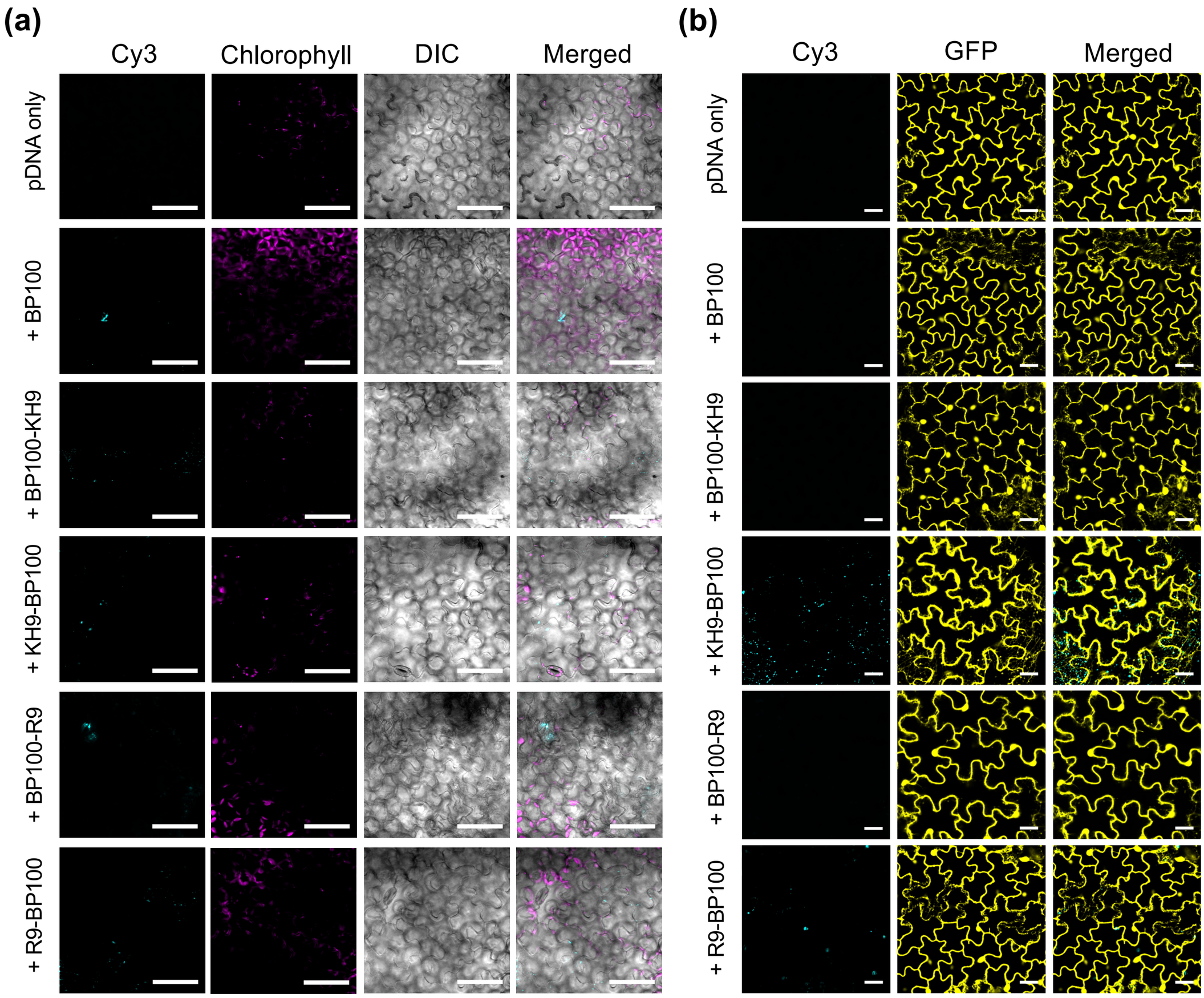

Figure S10. Internalization of Cy3-labeled pDNA/CPP complexes to plant cells
(a) Internalization of different Cy3-labeled pDNA/CPP complexes in epidermal cells of soybean leaves at 2 hours post spraying. **(b)** Internalization of different Cy3-labeled pDNA/CPP complexes (cyan) in epidermal cells of transgenic leaves of tomato overexpressing GFP at 2 hours post spraying. GFP fluorescence was shown as yellow color in this figure. Scale bars = 50 μm.

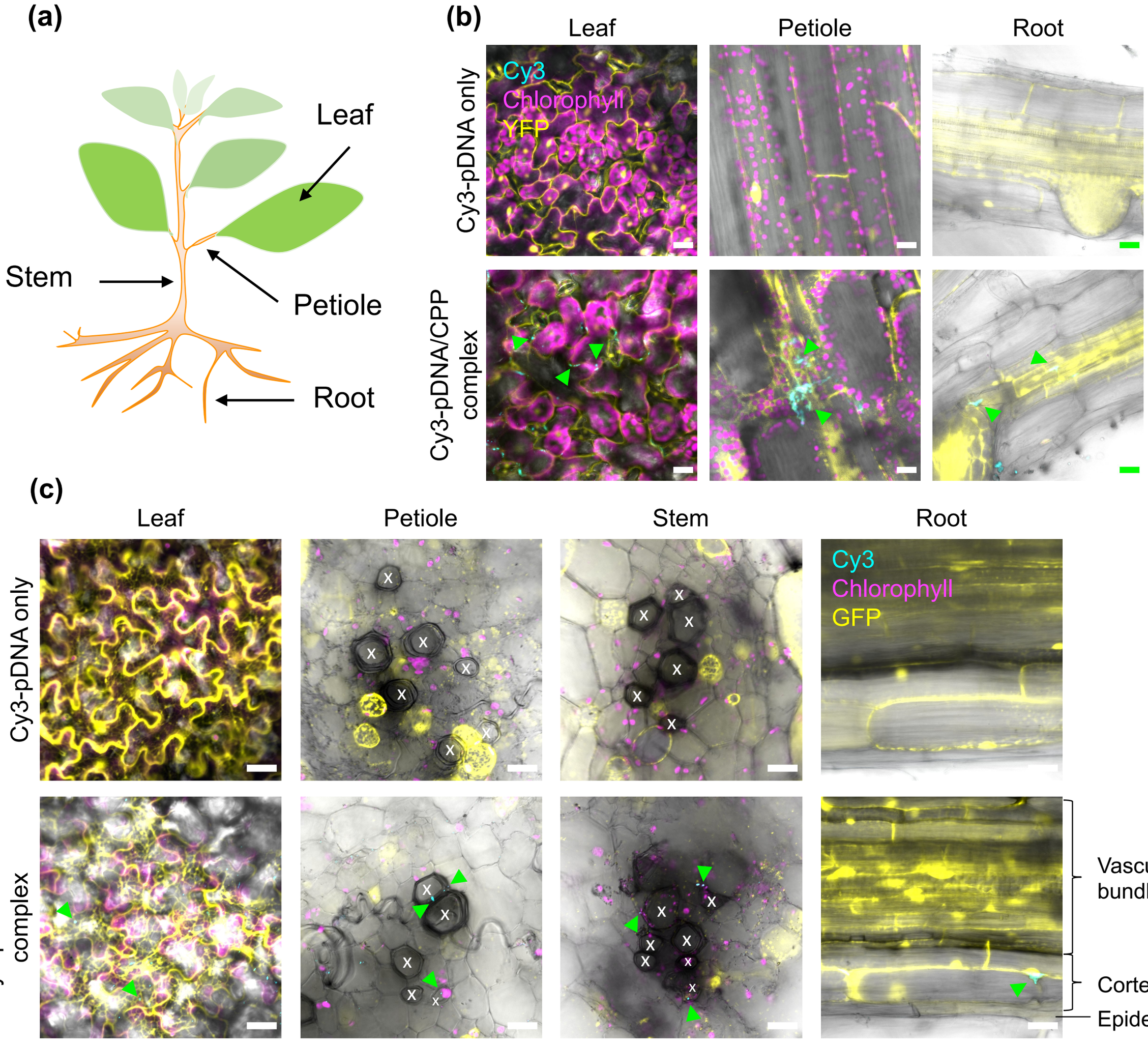

Figure S11. Long-distance translocation of Cy3-labeled pDNA/CPP complexes in plants. Fluorescence imaging of Cy3-labeled pDNA in leaf, petiole, stem, and root sections **(a)** of plants sprayed with solutions containing Cy3-pBI221 only and Cy3-pBI221/KH9-BP100 complexes formed at N/P ratio = 2.0 were performed to study translocation of pDNA/CPP complexes from leaves to the other plant tissues after 2 days of spraying. **(b)** Distribution of Cy3-labeled pDNA/CPP complexes in different tissues of YFP-overexpressing transgenic Arabidopsis after spray application. **(c)** Detection of Cy3 fluorescence in leaves, and vascular bundles of petioles, stems, and root of GFP-overexpressing tomatoes foliarly-sprayed by solutions containing Cy3-pDNA only and Cy3-pDNA/CPP complexes. Scale bars = 20 μm. Green arrows indicate the Cy3 fluorescence in **(b)** and **(c)**. X represents the xylem cells in vascular system of petiole and stem.

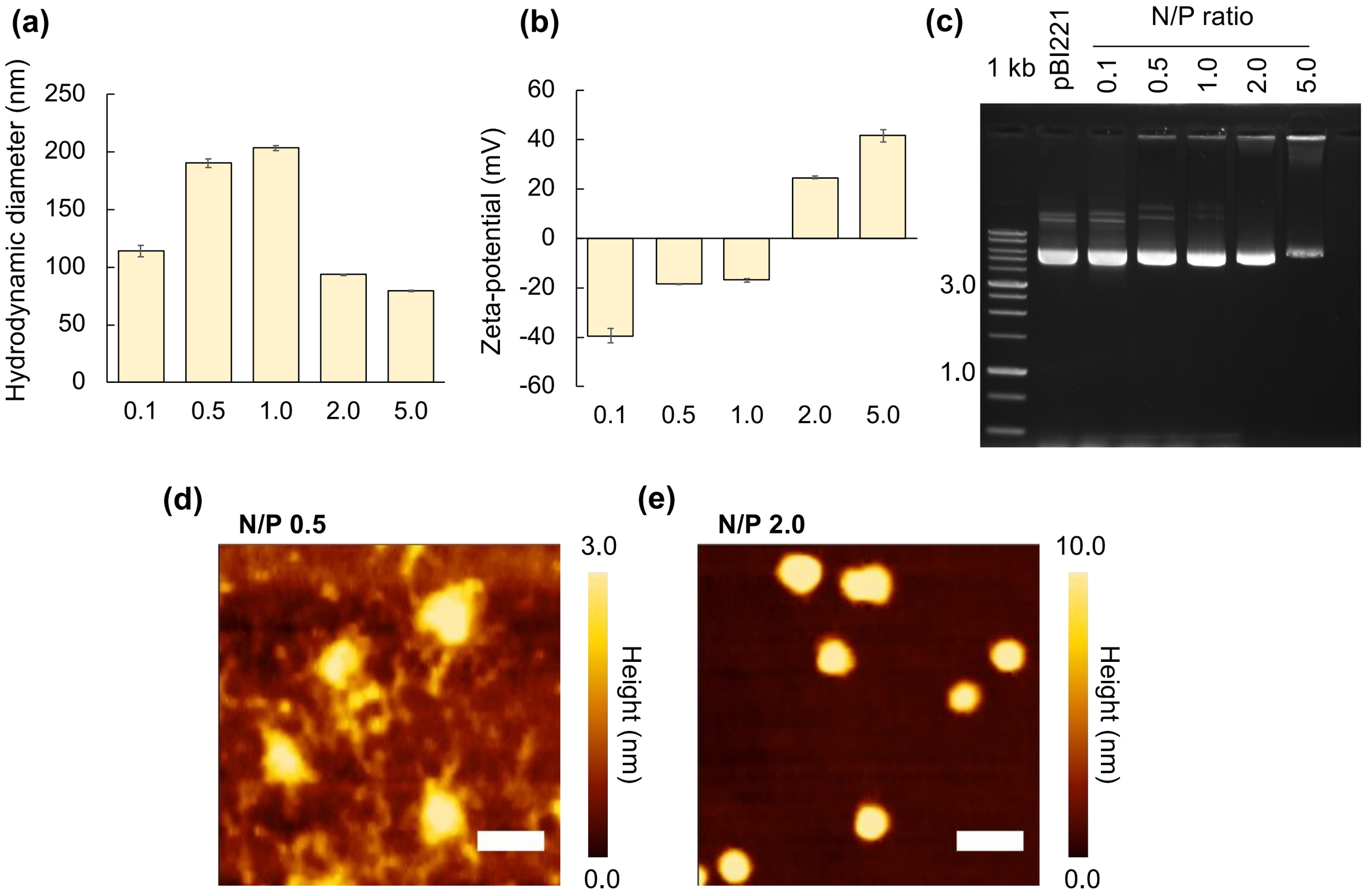

Figure S12. Formation of pBI221/KH9-BP100 complexes at different N/P ratios
(a) Hydrodynamic diameters and **(b)** surface charges (zeta-potential) of polydisperse pBI221/KH9-BP100 complexes formed at different N/P ratios in water. Error bar = standard deviation of average values from 4 experimental data. **(c)** Gel-electrophoretic mobility shift assay of pBI221/KH9-BP100 complexes formed at different N/P ratios. **(d)** and **(e)** Morphological appearances of pBI221/KH9-BP100 complexes formed at N/P ratio = 0.5 and 2.0 determined by tapping-mode AFM. Heat maps represent the height of complexes on mica surface. Scale bars = 200 nm.

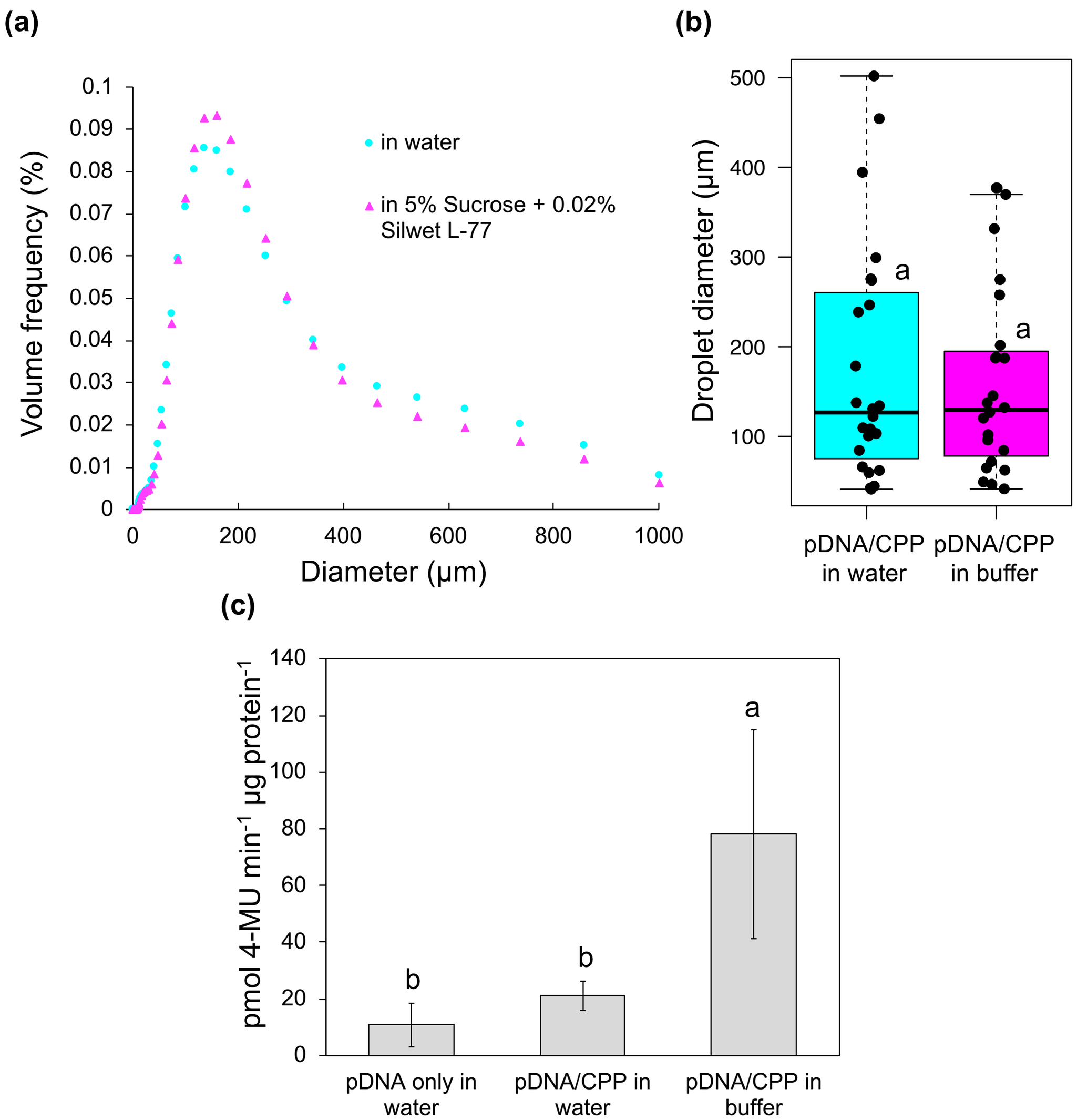

Figure S13. Droplet size and transfection efficiency of pBI221/KH9-BP100 complex in spray solution

(a) and **(b)** Average diameter **(a)** and distribution of droplet size **(b)** of pBI221/KH9-BP100 complex formed at N/P ratio = 2.0 in water and in 5% sucrose + 0.05% Silwet L-77 (as a spray solution). Dots in box plot (b) represent the distributed droplet sizes of solutions after spraying through the nozzle head of 5-ml atomizer (as shown in **Fig. 3**). Black bars indicate median of droplet diameters. Letter shows no-significant difference of droplet diameter of pDNA/CPP complex in water and in spray solution ("in buffer") analyzed by one-way ANOVA with Tukey's HSD test at $p = 0.05$. **(c)** GUS activity in Arabidopsis leaves at 24 hours after spraying with different solutions containing pDNA/CPP complexes. Error bar = standard deviation of mean. Letters indicate significant differences of mean of GUS activity in different samples analyzed by one-way ANOVA with Tukey's HSD test at $p = 0.05$ ($n = 8$).

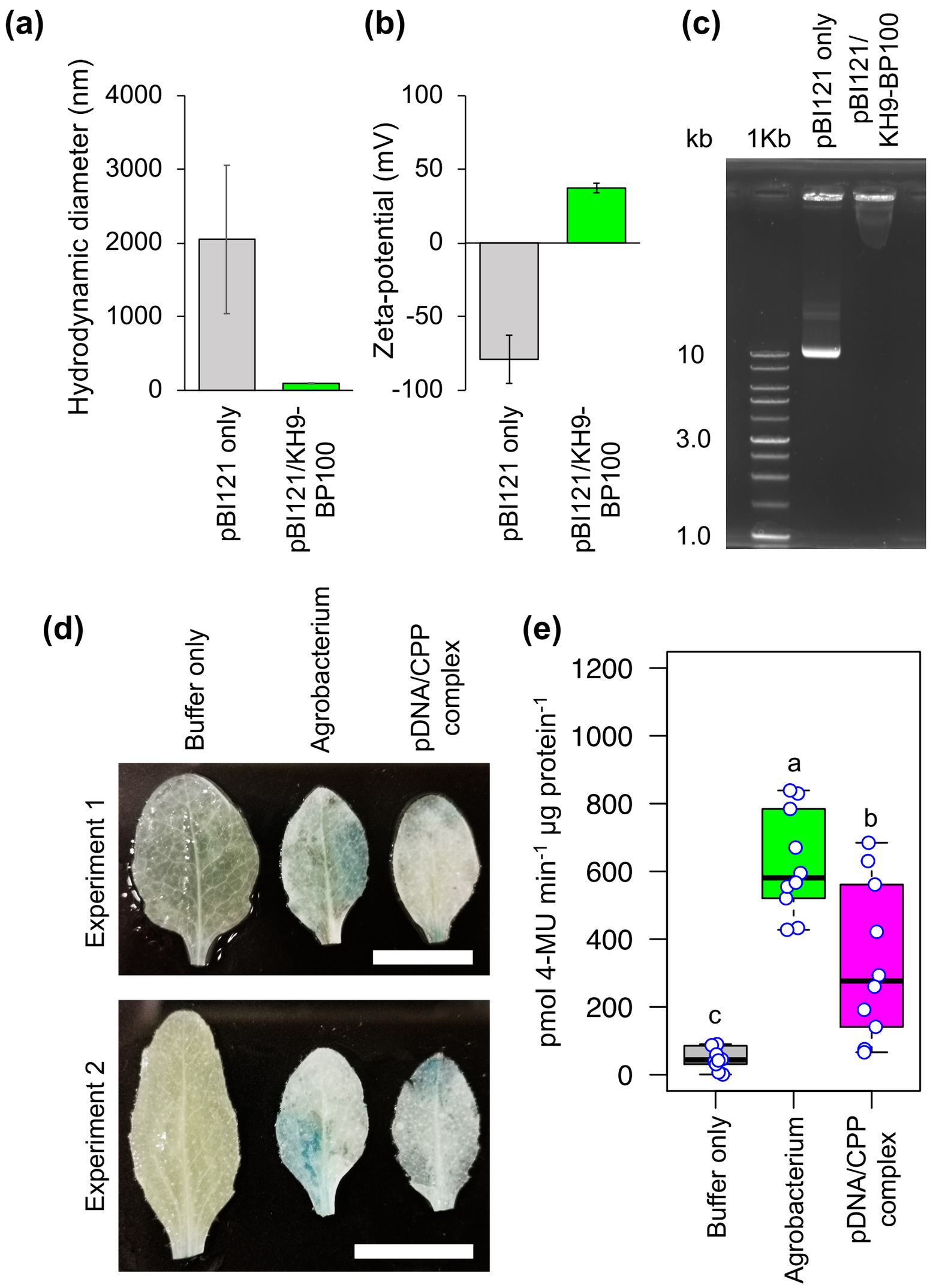

Figure S14. Comparison of transfection efficiencies between Agrobacterium-based and peptide carrier-mediated plasmid DNA delivery to plants *via* foliar spraying
Plant binary vector; pBI121, harboring GUS expression cassette was formed pDNA/CPP complexes with KH9-BP100 at N/P ratio = 2.0. (**a**) Particle size and (**b**) surface charge of pBI121/KH9-BP100 complex formed at N/P ratio = 2.0. Error bars = standard deviations of average values from 5 replicates (**c**) Gel mobility shift assay of pBI121/KH9-BP100 complexes formed at N/P ratio = 2.0. After complex formation, Arabidopsis (Col-0) plants were sprayed with spray solutions (5% sucrose + 0.05% Silwet L-77) containing either pDNA/CPP complexes or *Agrobacterium tumefaciens* str. LBA4404 harboring pBI121 (OD_{600nm} = 1.0). (**d**) Histochemical staining of GUS catalytic activity on plant leaves at 1 DAS. Scale bars = 1.0 cm. (**e**) Enzymatic activity of GUS reporter protein in Arabidopsis leaves after spraying with Agrobacterium harboring pBI121 or pBI121/KH9-BP100 complexes at 1 DAS. GUS activities in 10 plant leaves from 2 independent spray experiments were presented as box plot with data distribution (blue circles). Black bars represent medians of GUS activity in each treatment. Letters indicate statistically significant differences in GUS activity (one-way ANOVA with Tukey's HSD test, p = 0.001).

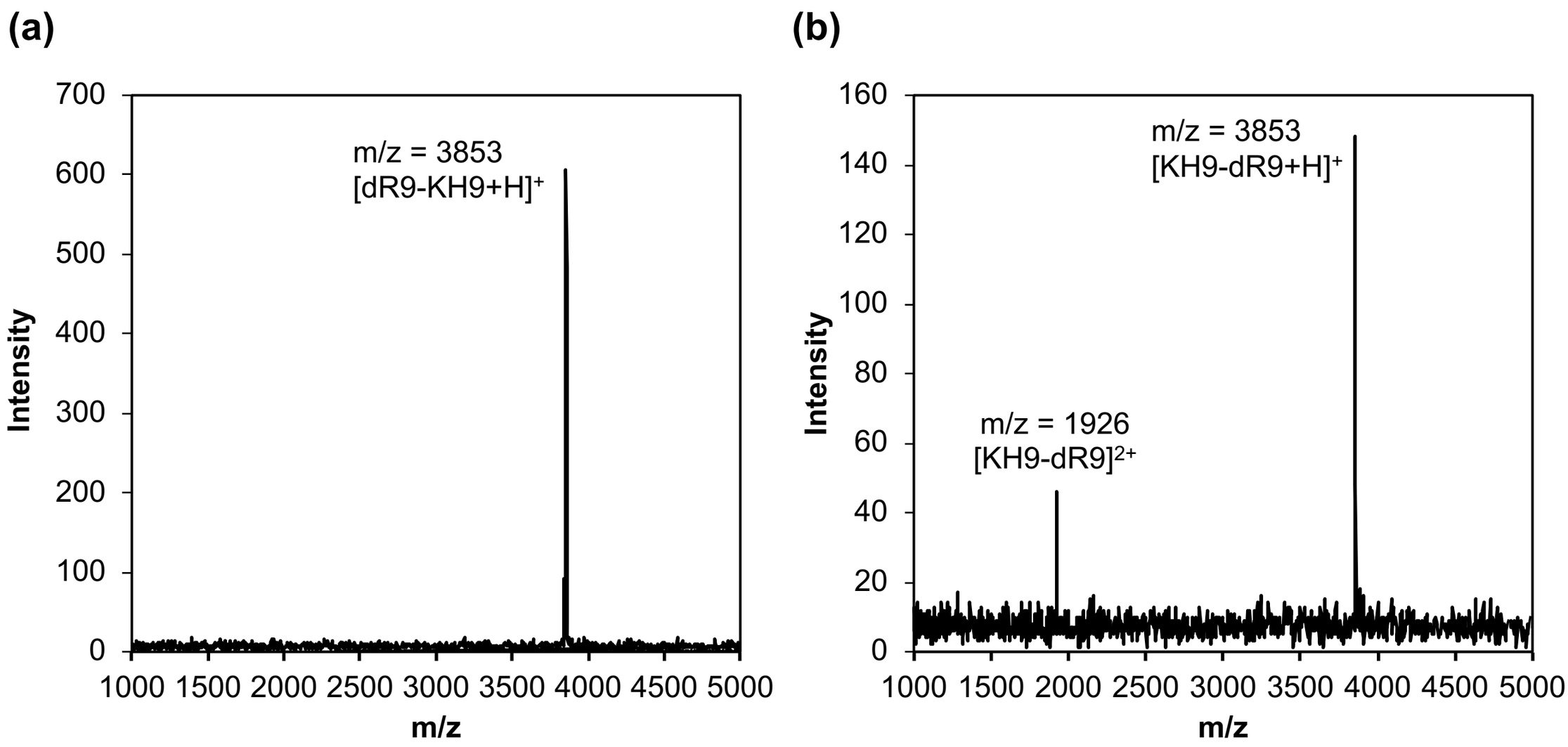

Figure S15. MALDI-TOF mass spectra of (**a**) dR9-KH9 and (**b**) KH9-dR9

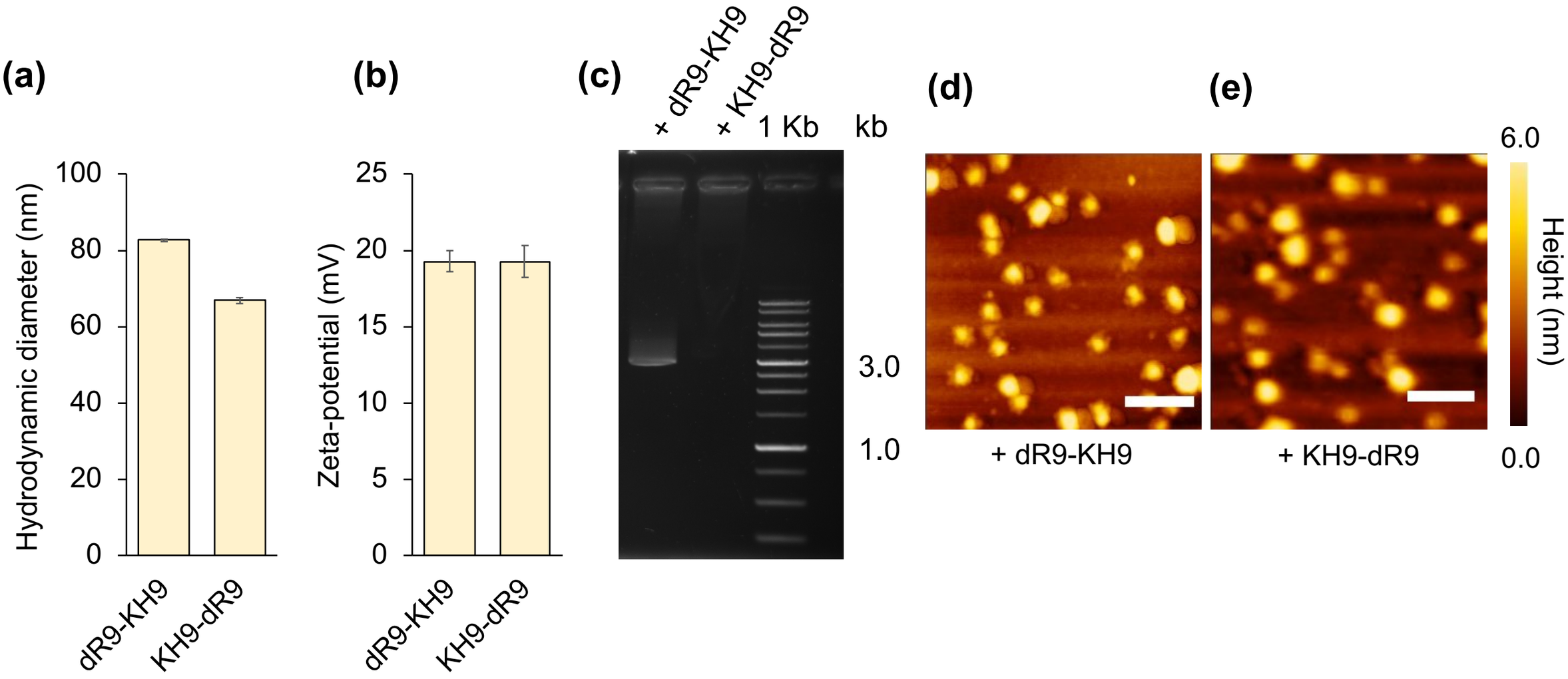

Figure S16. Physicochemical properties of different Cy3-labeled pBI221/CPP complexes formed with dR9-KH9 and KH9-dR9 at N/P ratio = 2.0

(a) Hydrodynamic diameter and **(b)** zeta-potential of different Cy3-labeled pBI221/CPP complexes formed at N/P ratio = 2.0. Error bars = SD of average values (*n* = 5). **c)** Agarose gel mobility shift assay of different Cy3-labeled pBI221/CPP complexes formed at N/P ratio = 2.0. **(d)** and **(e)** AFM images of complexes between Cy3-labeled pBI221 and dR9-KH9 **(d)** and KH9-dR9 **(e)** on the mica surface. Heat map represents the height of complexes and scale bars is 200 nm.

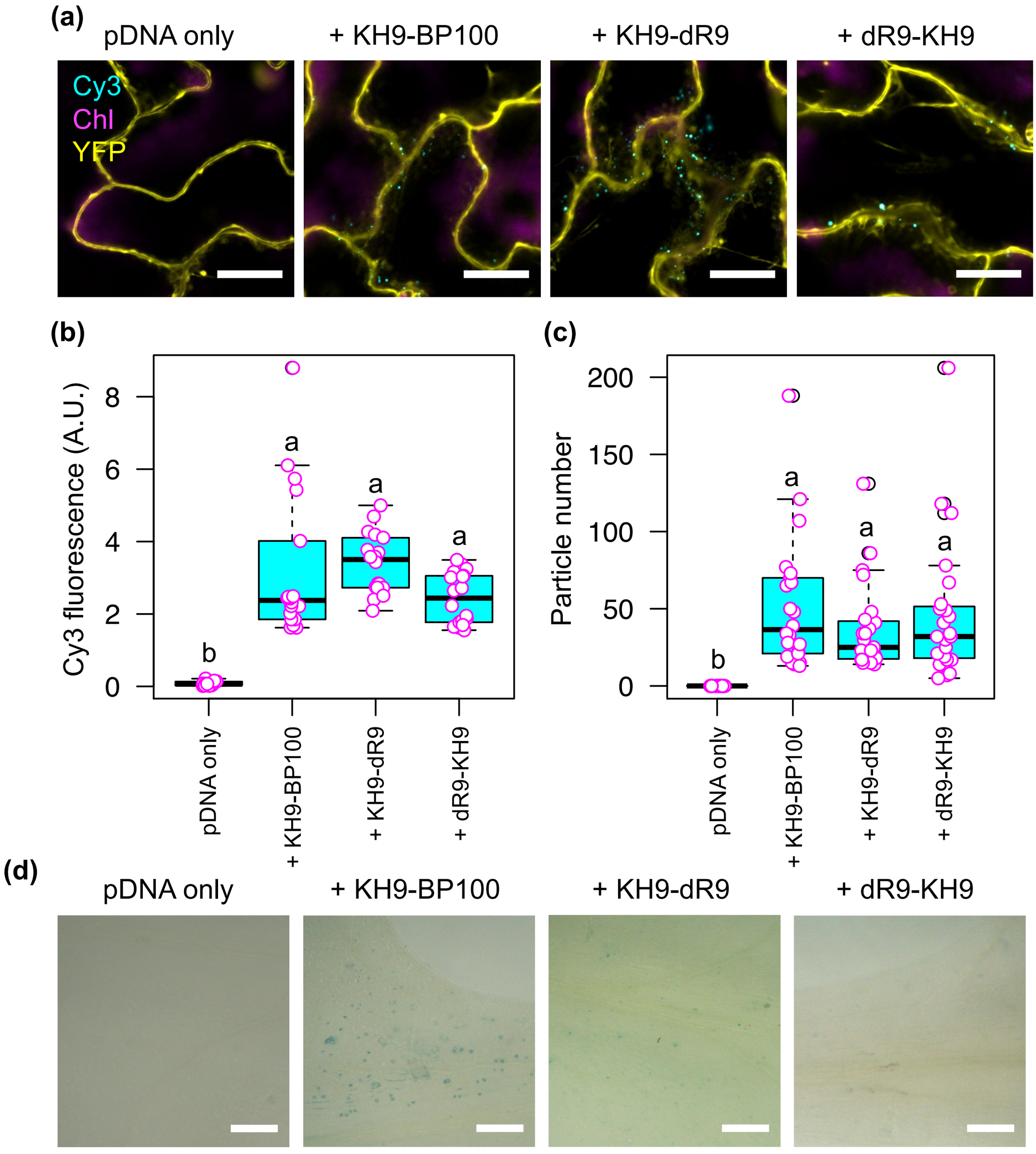

Figure S17. Internalization of Cy3-labeled pBI221 mediated by different KH9-fused CPPs **(a)** Internalization of different Cy3-lebeled pBI221/CPP complexes (N/P ratio = 2.0) in epidermal cells of YFP-overexpressing Arabidopsis leaves at 2 hours post spraying. Chl = chlorophyll autofluorescence. Scale bars = 50 μm. **(b)** Distribution of Cy3 fluorescent intensities in epidermal cells of Arabidopsis leaves as in box plot. The experiments were repeated three times. Cy3 fluorescent intensities were determined from 18 ROIs (6 ROIs per experiments, *n* = 18) collected at 2 hours post spraying with different Cy3-labeled pBI221/CPP complexes. Black bars are medians of the distributed data. **(c)** Different number of Cy3-labeled particles formed inside the plant cells sprayed by different Cy3-labeled pBI221/CPP complexes. Distributions of Cy3 fluorescent intensities and particle number in plant cells after spraying with different Cy3-labeled pBI221/CPP complexes were represented as box plot. Data distribution in each treatment was shown by dots (in 24 ROIs from 3 independent samples per treatments, *n* = 24) and black bars indicated median of the distributed data. Different letters in box plot show statistical significant differences of means of values as analyzed by one-way ANOVA with Tukey's HSD test at *p* = 0.05. **(d)** GUS activity of Arabidopsis leaves at 24 hours post spraying with different pBI221/CPP complexes formed at N/P ratio = 2.0. Scale bars = 500 μm.

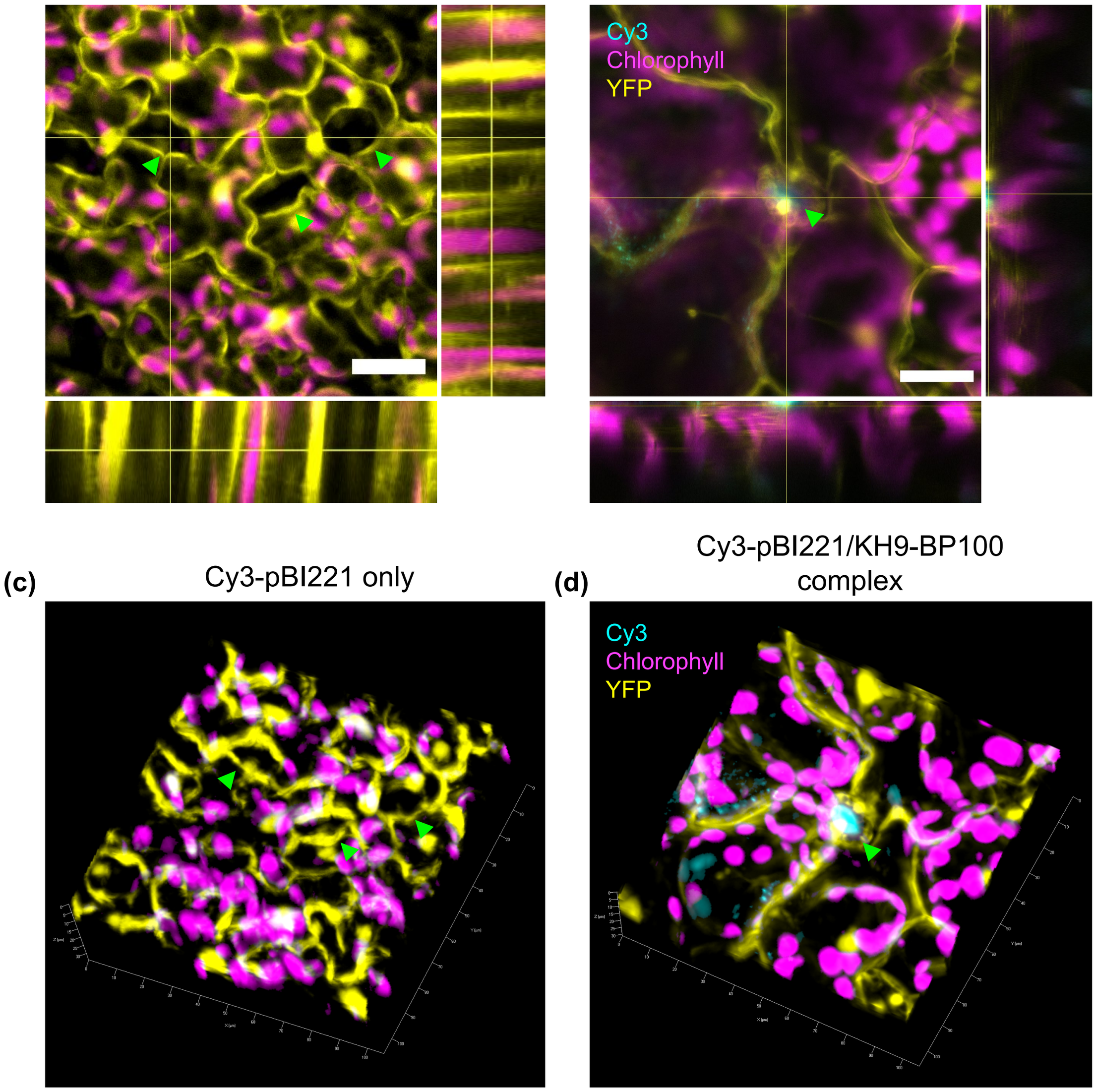

Figure S18. Stomatal uptake of Cy3-labeled pDNA/CPP complex to plant cells
Uptake of Cy3-labled pBI221/KH9-BP100 complexes formed at N/P ratio = 2.0 to YFP-overexpressing Arabidopsis leaf was observed under CLSM at 2 hours post spraying. **(a)** Z-stacked images (100 slices) of plant leaf sprayed with a solution containing Cy3-labeled plasmid DNA only. **(b)** Z-stacked fluorescence images (81 slices) of plant leaf sprayed with a solution containing Cy3-pBI221/KH9-BP100. Scale bars = 20 μm. **(c)** and **(d)** Distribution of Cy3-labeled pDNA/CPP complexes in plant leaf after spraying with Cy3-pDNA only **(c)** and Cy3-pDNA/CPP complexes **(d)**. The z-stacked fluorescence images in **(a)** and **(b)** were rendered to create (~ 30 μm) 3-dimentional models of leaf cell layers that consist of the guard cells (indicated by green arrows), epidermal cells, and palisade mesophylls.

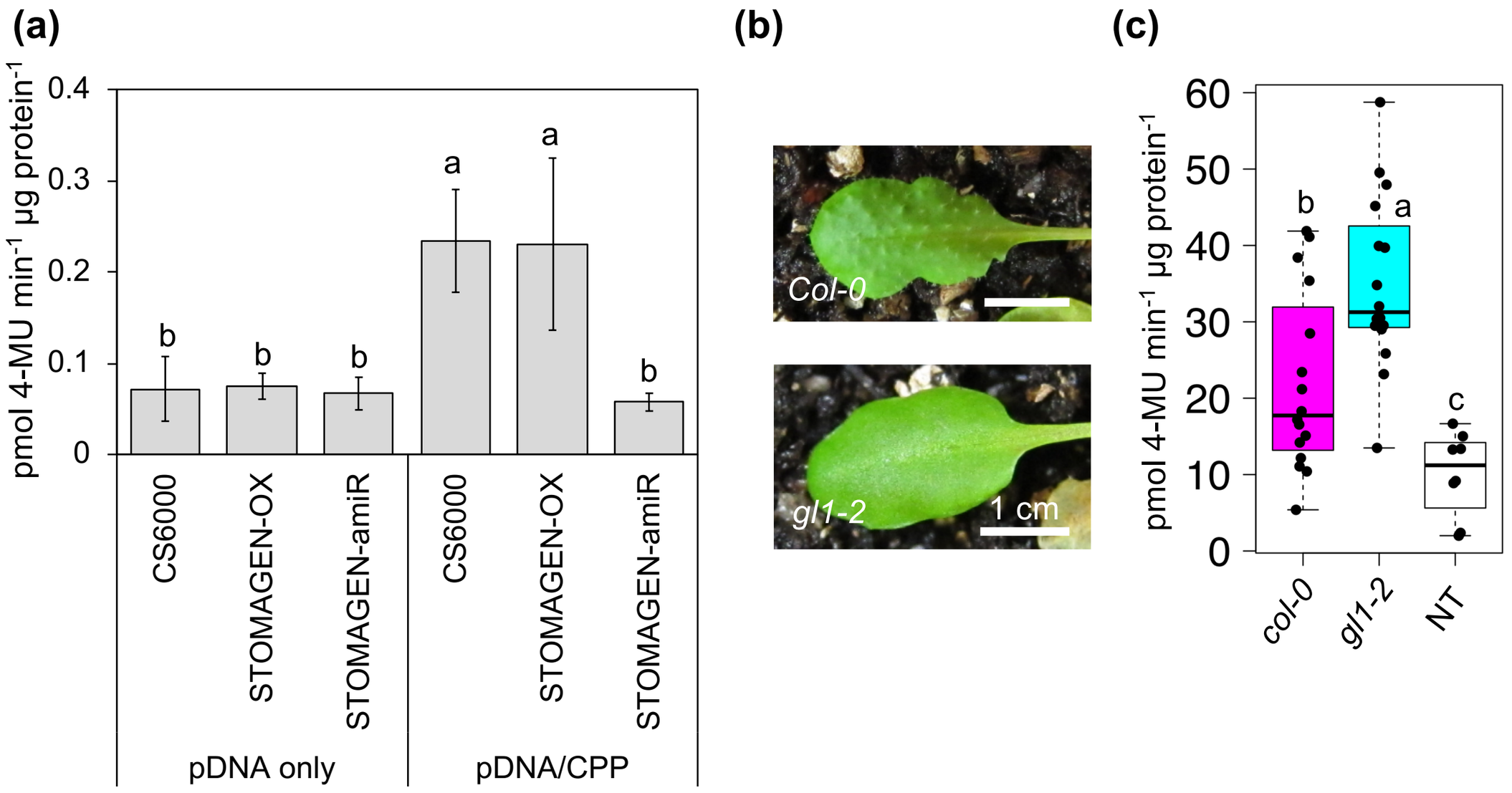

Figure S19. Roles of stomata and leaf trichome on transfection efficiencies of pBI221/KH9-BP100 complexes

(a) GUS activities in transgenic Arabidopsis leaves with different numbers of stomata after spraying with pDNA/CPP complexes. CS6000, wild type; STOMAGEN-OX, transgenic plant with numerous stomata; STOMAGEN-amiR, transgenic line with no stomata. Error bars = standard deviation (SD) (n = 4) **(b)** Appearance of trichomes on the leaf surface in *A. thaliana* ecotype Columbia-0 (Col-0) and the trichrome-less mutant *gl1-2*. **(c)** Distribution of GUS activities in *A. thaliana* leaves with and without trichomes after spraying with pDNA/CPP complexes is shown as a box plot. NT, non-transfected Col-0 leaves. Black bars represent medians of GUS activity. Dots represent individual data points (n = 18 for Col-0 and *gl1-2*, n = 10 for NT)). Different letters indicate significant differences in GUS activity, as analyzed by one-way ANOVA with Tukey's HSD test at p = 0.05.

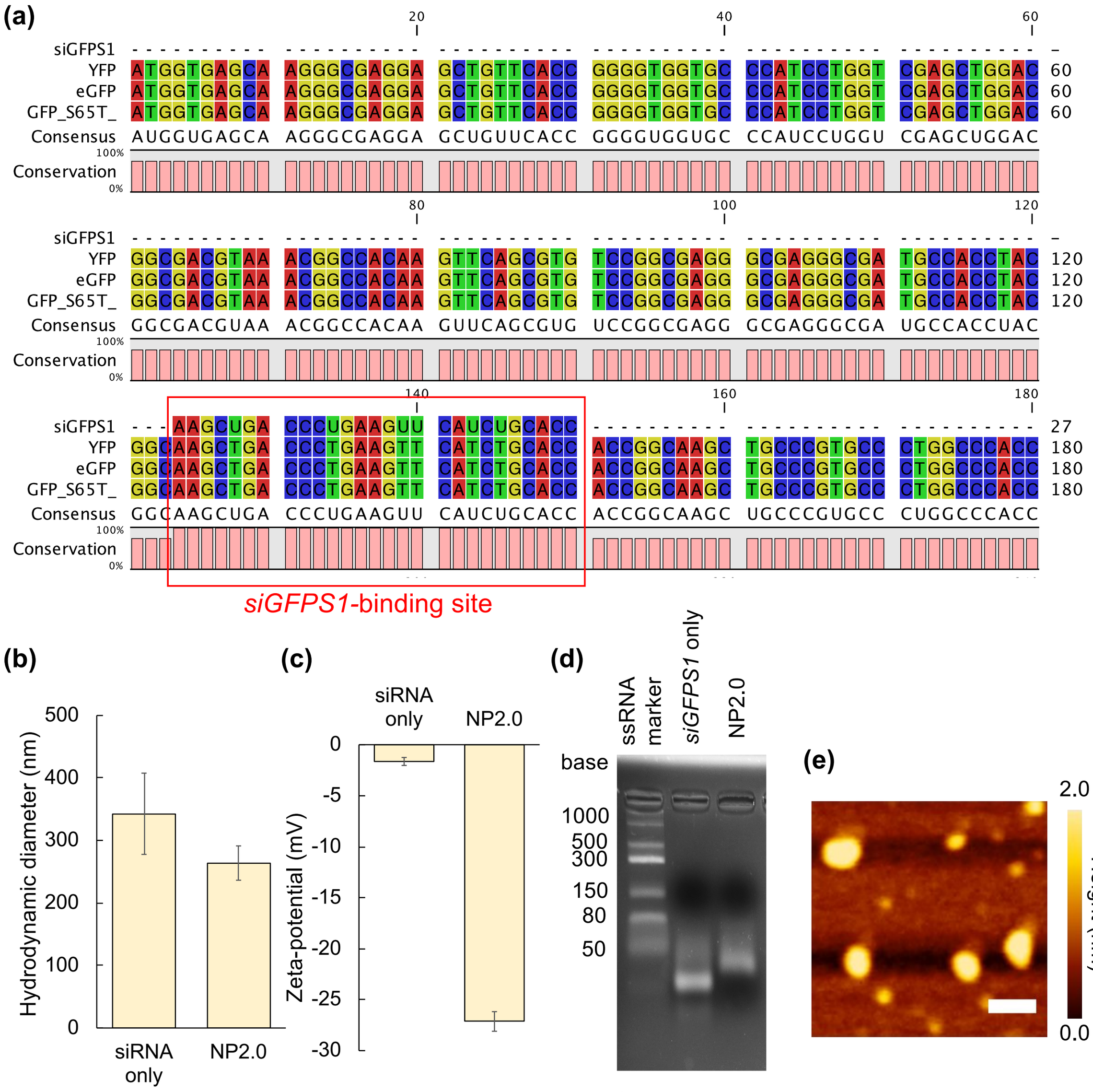

Figure S20. Formation of *siGFPS1*/KH9-BP100 complexes for suppression of GFP expression in plant cells

(a) Multiple sequence alignment of the sense strand of *siGFPS1* and *eGFP*, *GFP(S65T)* and *YFP* nucleic acid sequences. This result indicates that *siGFPS1* can potentially recognize its binding sequences of different transcripts of GFP variants (red rectangle). **(b)** hydrodynamic diameter and **(c)** zeta-potential of *siGFPS1*/KH9-BP100 complexes formed at N/P ratio = 2.0. Error bars = SD of average data (*n* =4). **(d)** Gel-retardation assay of siGFPS1/KH9-BP100 complexes formed at N/P ratio = 2.0. **(e)** AFM image of *siGFPS1*/KH9-BP100 complexes formed at NP ratio = 2.0. Heat map represents the height of complex on mica surface. Scale bar = 500 nm.

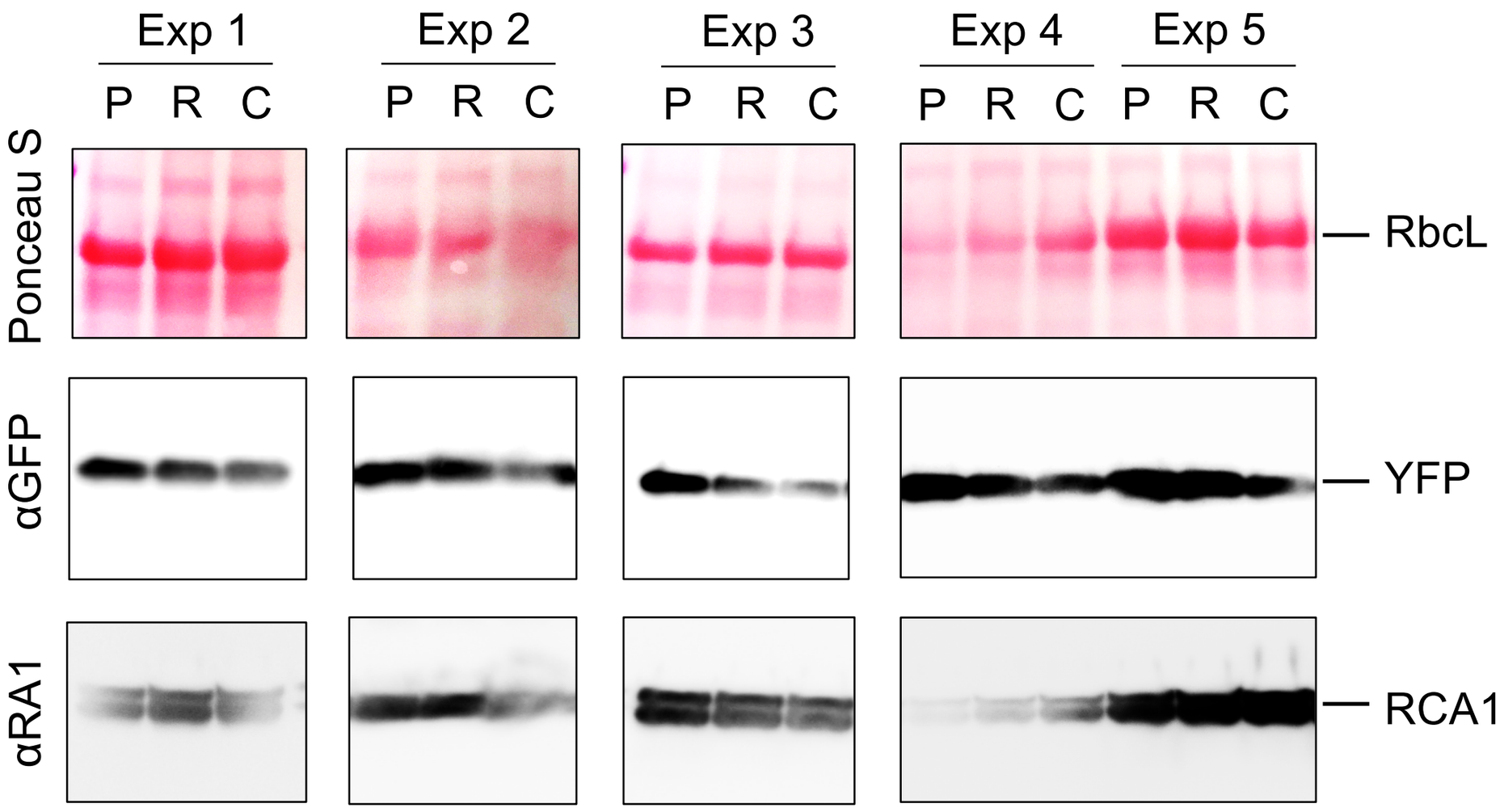

Figure S21. Western blot results of total leaf proteins isolated from transgenic Arabidopsis leaves sprayed with *siGFPS1*/KH9-BP100 complex at 3 DAS
Western blot experiments were performed 5 times with biologically independent samples. P = KH9-BP100 only-sprayed leaves, R = *siGFPS1* only-sprayed leaves, C = total proteins from leaves sprayed with *siGFPS1*/KH9-BP100 complex. Exp = experimental number. RbcL = Rubisco large subunit. RCA1 = RubisCo Activase 1 protein.

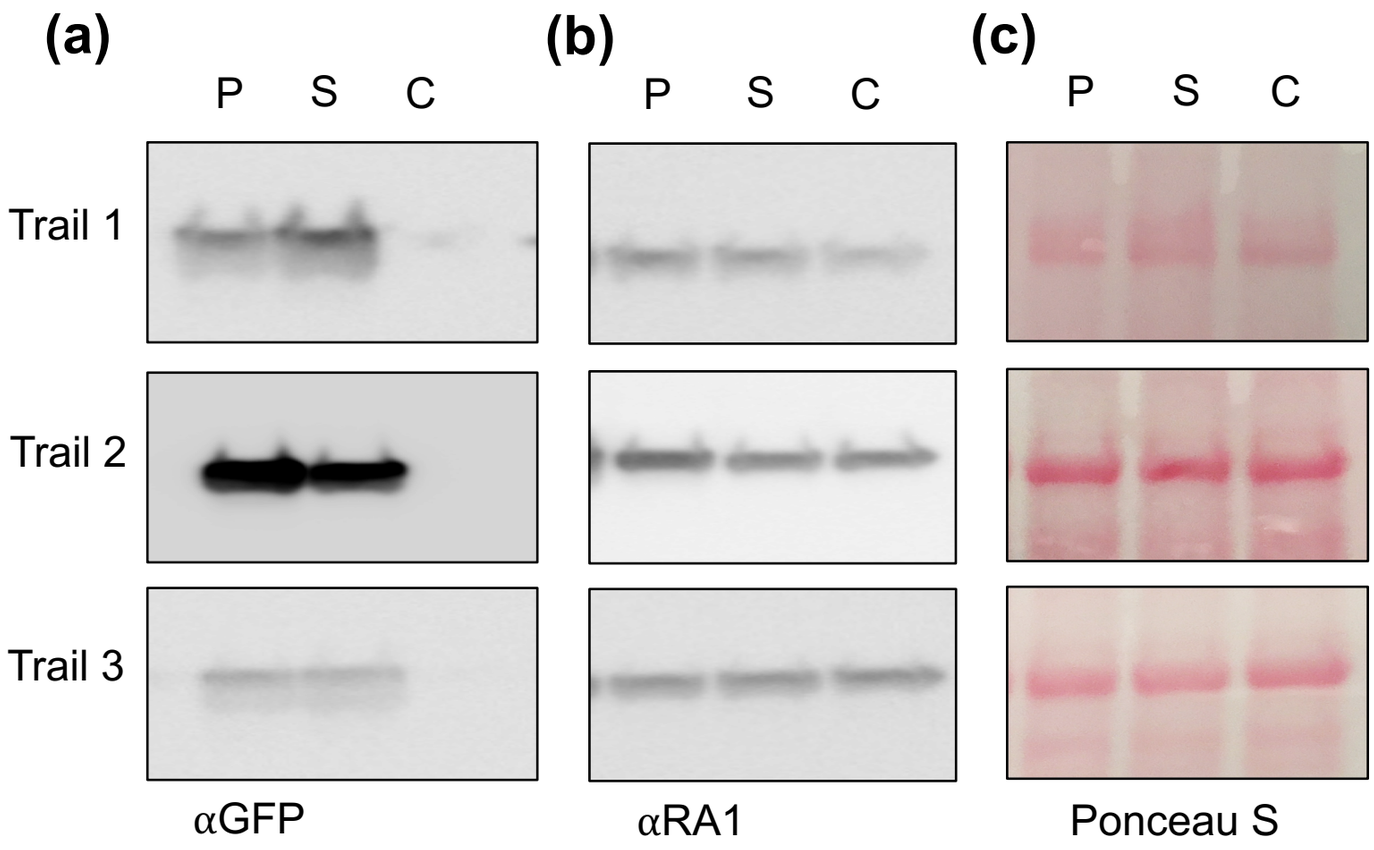

Figure S22. Western blot results of total leaf proteins isolated from transgenic GFP-overexpressing tomato leaves sprayed with *siGFPS1*/KH9-BP100 complex at 3 DAS
(a) Immunoblotting with anti-GFP polyclonal antibody. **(b)** Immunoblotting with anti-RA1 polyclonal antibody **(c)** Ponceau S staining of highly redundant Rubisco large subunit protein on membrane. Immunoblot analyses were performed in leaf protein samples from 3 independent spray experiments. P = KH9-BP100 only-sprayed leaves, R = *siGFPS1* only-sprayed leaves, C = total proteins from leaves sprayed with solutions containing *siGFPS1*/KH9-BP100 complexes.

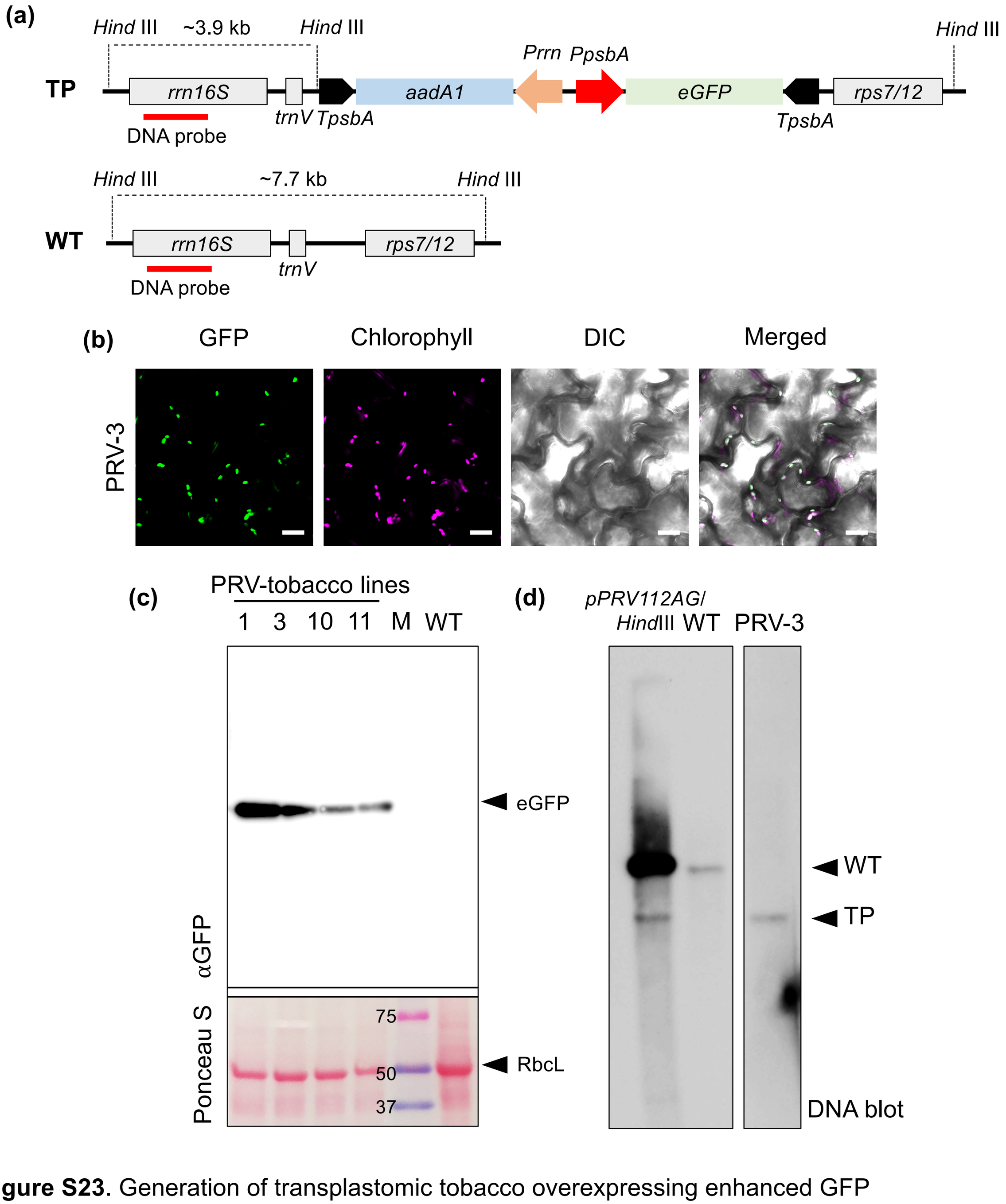

Figure S23. Generation of transplastomic tobacco overexpressing enhanced GFP
(a) Transplastomic tobacco lines were regenerated from *enhanced (e)GFP*-expression vector-coated AuNPs-based particle-bombarded tobacco leaves (TP; transplastomic plant, WT; Wild type). **(b)** Successful transformants were screened by CLSM observation to detect the eGFP fluorescence in chloroplasts. Scale bars = 20 μm. **(c)** Immunoblotting of eGFP expression in transplastomic PRV lines. M = protein molecular marker with molecular weight (kDa). **(d)** Transplastomic lines (PRV-3) with high eGFP fluorescence were confirmed its stable, homoplastomic chloroplast genetic background (“homoplasmic”) by DNA blot analysis. A lower molecular weight DNA band indicates the homologous recombination of *eGFP*-gene expression cassette to the DNA of chloroplasts.

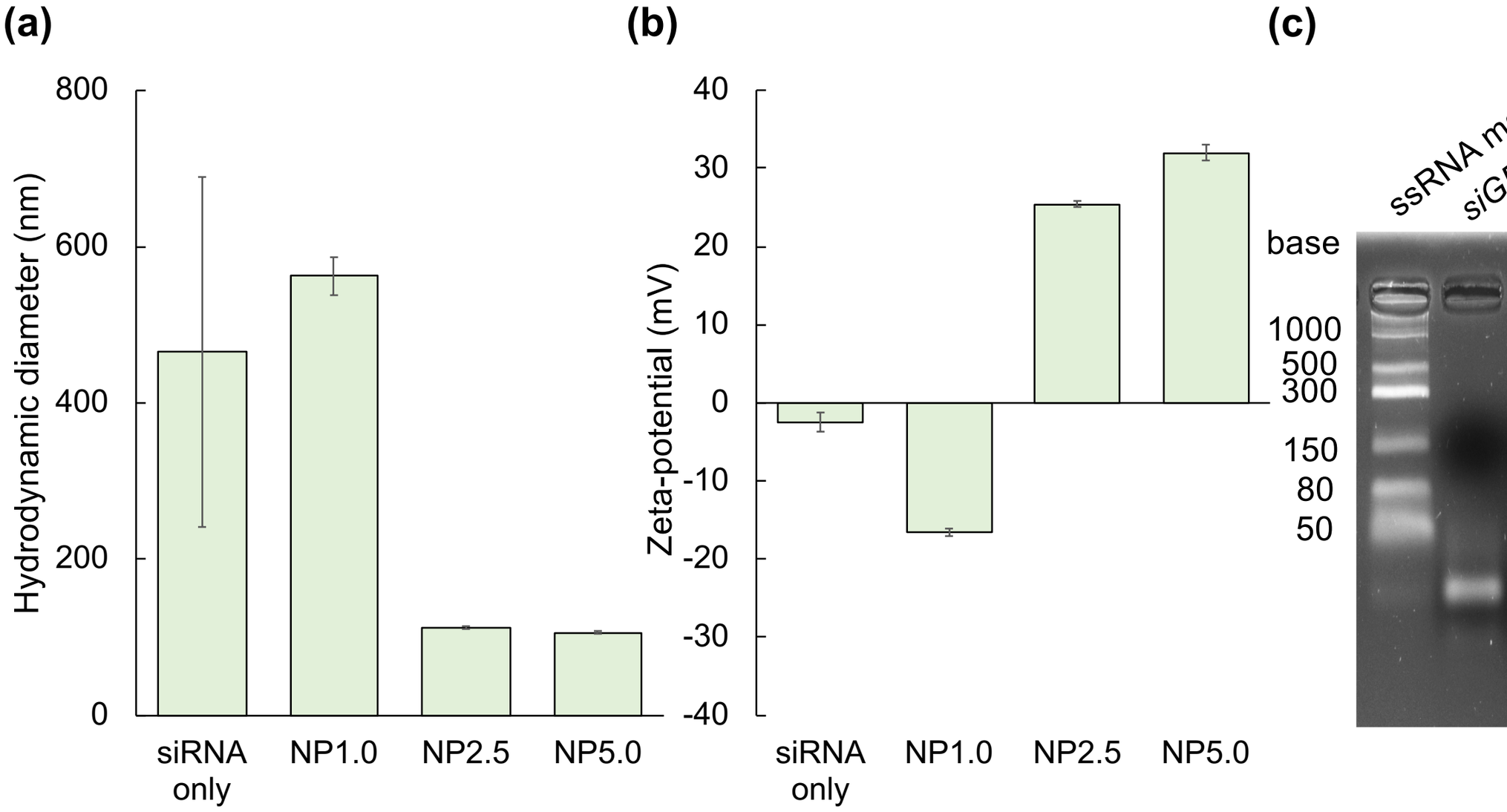

Figure S24. Formation of clustered *siGFPS1*/KH9-OEP34/BP100 complexes for targeted siRNA delivery to chloroplasts in plant cells

(a) Hydrodynamic diameter and **(b)** surface charge of the clustered siRNA/CTP/CPP complexes formed at different N/P ratios. Error bar represents standard deviation of the average values (n = 5). **(c)** Agarose gel mobility shift assay of *siGFPS1*/KH9-OEP34/BP100 complexes formed at different N/P ratios. **(d)** to **(f)** Morphological appearances of the clustered *siGFPS1*/KH9-OEP34/BP100 complexes formed at N/P ratios = 1.0 to 5.0 under the AFM observation. Heat map represents the height of complexes on the mica surface. Scale bars = 200 nm.

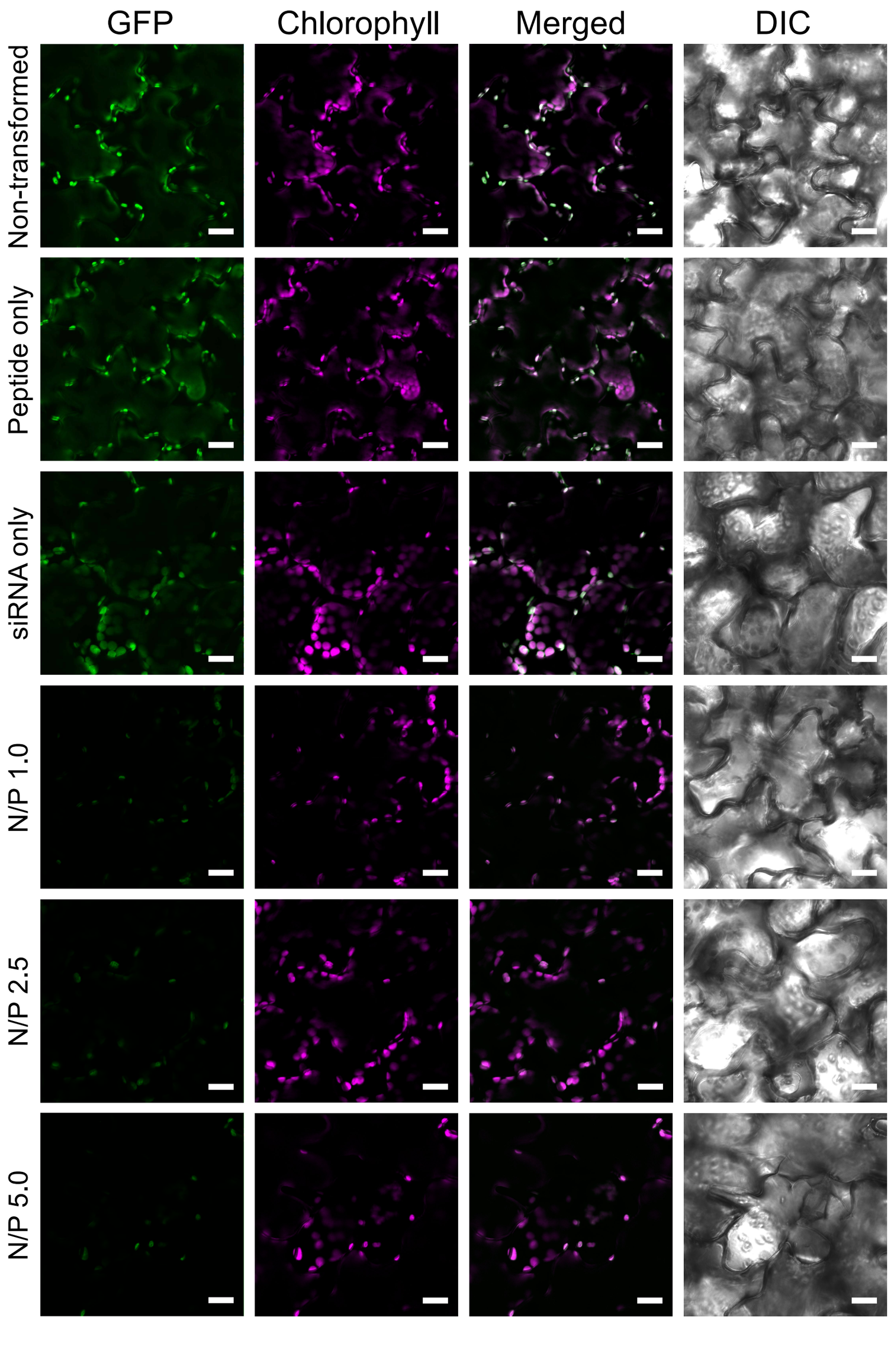

Figure S25. Representative fluorescent images of chloroplast-specific GFP in transplastomic tobacco leaf cells spray-transfected with the clustered siRNA/CTP/CPP complexes
Fully-expanded transplastomic tobacco leaves overexpressing eGFP specifically in chloroplasts were sprayed by solutions containing clustered siRNA/peptide complexes formed at different N/P ratios. GFP fluorescence in chloroplasts was observed under confocal laser-scanned microscope at 3 DAS. Scale bars = 20 μm.

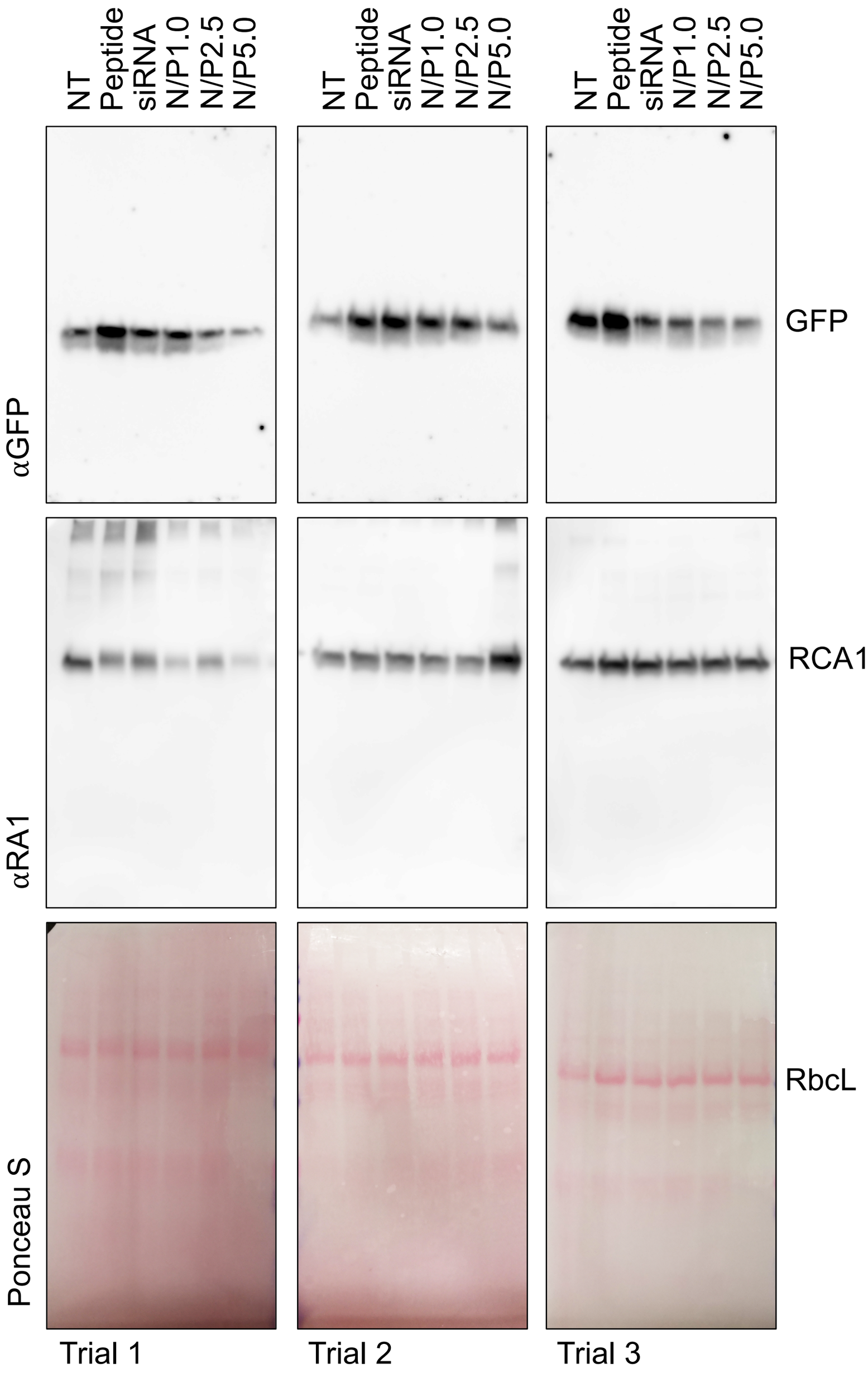

Figure S26. Immunoblot analyses of eGFP accumulation in transplastomic tobacco leaves overexpressing eGFP in chloroplasts after spraying with siRNA/peptide complexes
Total leaf proteins were extracted from plant leaves and blotted against anti-GFP and anti-RA1 polyclonal antibodies to detect differential accumulation of eGFP in plant leaves after spraying with solutions containing *siGFPS1*/KH9-OEP34/BP100 complexes formed at different N/P ratios. Lower panel shows the membrane staining with Ponceau S to confirm equal loading of total leaf proteins on the membrane (indicated by similar intensities of RbcL bands on membrane). The western blotting experiments were performed using leaf samples collected from 3 biological independent experiments.

Table S1. CPPs and CTP used in this study

CPP name	Sequence (N → C)	Biomolecule conjugates	Mw (kDa)	Net charge at pH 7.0	Reference
TAMRA-labeled CPPs					
BP100	KKLFKKILKYL	TAMRA	1.83	5.0	14
KH9	KHKHKHKHKHKHKHKHKH	TAMRA	2.82	11.0	
R9	RRRRRRRRR	TAMRA	1.84	9.0	
d-R9	d-(RRRRRRRRR)	TAMRA	1.84	9.0	
KAibA	$(Lys(Aib)Ala)_5$[a]	TAMRA	1.98	n.d.	29
KAibK	$(Lys(Aib)Lys)_4$[a]	TAMRA	2.07	n.d.	
KAibG	$(Lys(Aib)Gly)_6$[a]	TAMRA	2.33	n.d.	
Cationic CPPs					
BP100	KKLFKKILKYL	-	1.42	4.0	25
BP100-KH9	KKLFKKILKYLKHKHKHKHKHKHKHKHKH	-	3.81	16.0	16,17
KH9-BP100	KHKHKHKHKHKHKHKHKHKKLFKKILKYL	-	3.81	16.0	
BP100-R9	KKLFKKILKYLRRRRRRRRR	-	4.23	18.0	This study
R9-BP100	RRRRRRRRRKKLFKKILKYL	-	4.23	18.0	
dR9-KH9	d-(RRRRRRRRR)KHKHKHKHKHKHKHKHKH		3.81	18.9	
KH9-dR9	KHKHKHKHKHKHKHKHKHd-(RRRRRRRRR)		3.81	18.9	
CTP					
KH9-OEP34	KHKHKHKHKHKHKHKHKHMFAFQYLLVM	-	3.65	11.0	26,27

[a]; Degrees of polymerization, *n.d.*; not determined

Table S2. Physicochemical properties of different Cy3-labeled pBI221/CPP complexes used in transfection studies after spraying in Arabidopsis, soybean, and tomato leaves

Sample	Plasmid DNA	Cationic CPP (μM)	N/P ratio	Hydrodynamic diameter (nm)[a]	Zeta-potential (mV)[a]	PdI[a]	pH of solution[b]	Plant materials
Cy3-pDNA only	Cy3-labeled pBI221 (2.56 nM)	No CPP	0	745.3 ± 295.9	-25.0 ± 2.5	0.677 ± 0.036	7.74 ± 0.50	YFP-ox Arabidopsis, soybean (wild type), and GFP-ox tomato
BP100 complex		BP100 (6.5)	2.0	112.9 ± 1.9	-24.9 ± 1.3	0.264 ± 0.005	7.88 ± 0.17	
BP100-KH9 complex		BP100-KH9 (4.7)	2.0	75.9 ± 2.3	17.7 ± 1.6	0.375 ± 0.021	7.60 ± 0.24	
KH9-BP100 complex		KH9-BP100 (4.7)	2.0	77.0 ± 3.6	18.6 ± 2.3	0.395 ± 0.022	7.55 ± 0.31	
BP100-R9 complex		BP100-R9 (3.3)	2.0	54.1 ± 1.2	19.3 ± 5.3	0.223 ± 0.025	7.51 ± 0.41	
R9-BP100 complex		R9-BP100 (3.3)	2.0	74.1 ± 1.6	21.2 ± 0.7	0.370 ± 0.002	7.40 ± 0.27	
dR9-KH9 complex		dR9-KH9 (3.7)	2.0	82.6 ± 0.3	19.3 ± 0.7	0.211 ± 0.009	7.37 ± 0.19	
KH9-dR9 complex		KH9-dR9 (3.7)	2.0	66.8 ± 0.8	19.3 ± 1.0	0.379 ± 0.008	7.32 ± 0.30	

[a]; Determined by DLS measurement with Zeta-Nanosizer
[b]; Determined by pH meter

Table S3. Formulation and physicochemical properties of pBI221/KH9-BP100 complexes at various N/P ratios

N/P ratio	pBI221 (nM)	KH9-BP100 (μM)	Hydrodynamic diameter (nm)[a]	Zeta-potential (mV)[a]	PdI[a]	pH of solution[b]	Plant materials
0.1	2.56	0.233	113.8 ± 4.9	-39.4 ± 2.9	0.390 ± 0.010	7.63 ± 0.25	Wild type soybean leaves
0.5	2.56	1.17	190.1 ± 3.7	-18.6 ± 0.2	0.296 ± 0.051	7.63 ± 0.37	
1.0	2.56	2.33	203.2 ± 2.2	-17.0 ± 0.7	0.223 ± 0.019	7.75 ± 0.09	
2.0	2.56	4.66	93.2 ± 0.6	24.7 ± 0.6	0.121 ± 0.004	7.42 ± 0.15	
5.0	2.56	11.7	79.2 ± 0.6	41.6 ± 2.5	0.297 ± 0.024	6.61 ± 0.24	

[a]; Determined by DLS measurement with Zeta-Nanosizer
[b]; Determined by pH meter

Table S4. Physicochemical properties of pBI121/KH9-BP100 complexes used in comparison of transfection efficiency between pDNA/CPP complex and Agrobacterium

Sample	Plasmid DNA	Cationic CPP (μM)	N/P ratio	Hydrodynamic diameter (nm)[a]	Zeta-potential (mV)[a]	PdI[a]	pH of solution[b]	Plant materials
pDNA only	**pBI121 (5.21 nM)**	No CPP	0	2048.4 ± 1007.0	-78.9 ± 16.4	1.00 ± 0.02	9.11 ± 0.50	*Arabidopsis thaliana* (Col-0)
pBI121/KH9-BP100 complex		KH9-BP100 (9.4)	2.0	95.1 ± 6.7	37.4 ± 3.2	0.35 ± 0.03	8.05 ± 0.39	

[a]; Determined by DLS measurement with Zeta-Nanosizer
[b]; Determined by pH meter

Table S5. *siGFPS1* RNA sequences

siRNA	Sequence (5’ → 3’)	Direction	Target transcript
siGFPS1_S	AAGCUGACCCUGAAGUUCAUCUGCACC	Sense-strand	*GFP, eGFP, YFP*
siGFPS1_AS	GGUGCAGAUGAACUUCAGGGUCAGCUU	Antisense-strand	

Table S6. Physicochemical characteristics of *siGFPS1*/KH9-BP100 complexes formed at N/P ratio = 2.0 for gene suppression studies after spraying

Sample	*siGFPS1* (nM)	KH9-BP100 (μM)	N/P ratio	Hydrodynamic diameter (nm)[a]	Zeta-potential (mV)[a]	PdI[a]	pH of solution[b]	Plant materials
siRNA only	217.6	0	0	342.7 ± 65.0	-1.64 ± 0.39	0.67 ± 0.21	7.41 ± 0.16	YFP-ox Arabidopsis, GFP-ox tomato
siRNA/CPP complex	217.6	1.05	2.0	263.9 ± 27.5	-27.1 ± 0.96	0.70 ± 0.03	7.80 ± 0.27	

[a]; Determined by DLS measurement with Zeta-Nanosizer
[b]; Determined by pH meter

Table S7. Physicochemical properties of *siGFPS1*/KH9-OEP34/BP100 complexes for targeted gene suppression in chloroplasts of transplastomic tobacco overexpressing GFP after spraying

Sample	N/P ratio	*siGFPS1* (nM)	KH9-OEP34 (μM)	BP100 (μM)	Hydrodynamic diameter (nm)[a]	Zeta-potential (mV)[a]	PdI[a]	pH of solution[b]
siRNA only	0	217.6	0	0	465.4 ± 224.0	-2.45 ± 1.22	0.61 ± 0.34	7.97 ± 0.13
NP1.0	1.0	217.6	0.66	2.34	562.3 ± 24.5	-16.5 ± 0.48	0.53 ± 0.02	7.78 ± 0.25
NP2.5	2.5	217.6	1.32	4.68	112.7 ± 1.8	25.5 ± 0.39	0.37 ± 0.01	7.62 ± 0.31
NP5.0	5.0	217.6	3.30	11.7	106.6 ± 1.8	32.0 ± 1.01	0.38 ± 0.01	7.24 ± 0.10

[a]; Determined by DLS measurement with Zeta-Nanosizer
[b]; Determined by pH meter

Table S8. Plant materials, peptides, and nucleic acid cargos for foliar applications of biomolecules to plant nuclei and cytoplasm mediated by cell-penetrating peptides

Experiment	Plant materials	Functional peptides (μM)	Nucleic acids	Labeling	Purpose
Cell-penetration efficiencies of CPPs upon spraying	***A. thaliana*** (*eco.* Col-0) **Soybean** (cvs. Enrei, William-82, and Peking) **Tomato** (*mut*. MicroTom)	BP100 (54.6) KH9 (35.5) R9 (54.3) dR9 (54.3) KAibA (48.3) KAibK (50.5) KAibG (42.9)	none	5-carboxytetra-methylrhodamine (TAMRA) (chemical conjugation to either *N*- or *C*-terminal of CPP)	To determine cell-penetrating abilities of different TAMRA-labeled CPPs to plant leaf after foliar application
Transfection efficiencies of nucleic acid/CPP complexes after spraying	**YFP-ox *A. thaliana*** **Soybean** (cv. Enrei) **GFP-ox Tomato**	BP100 BP100-KH9 KH9-BP100 BP100-R9 R9-BP100 dR9-KH9 KH9-dR9	Cy3-labeled pBI221	Cyanine-3 (Cy3) (chemically cross-linked)	To study the internalization efficiencies and localization of various pDNA/CPP structures into plant cells
Foliar spraying of plasmid DNA/CPP complexes for transgene expression in plant cells	***A. thaliana*** (*eco.* Col-0, *mut. gl1-2*, STOMAGEN-OX, and STOMAGEN-amiR) **Soybean** (cv. Enrei)	KH9-BP100 dR9-KH9 KH9-dR9	pBI221	none	To elucidate gene expression function and role of leaf features on uptake of pDNA/CPP complexes
Gene silencing in plant cells mediated by the siRNA/CPP complex after foliar spraying	**YFP-ox *A. thaliana*** **GFP-ox Tomato**	KH9-BP100	*siGFPS1*	none	To study gene silencing activities of spray-induced siRNA/CPP complexes in plant cells

Table S9. Experimental materials for targeted deliveries of plasmid DNA and siRNA to chloroplasts *via* spray application of nucleic acid/peptide complexes

Experiment	Plant materials	Functional peptides	Nucleic acids	Purpose
Gene delivery to chloroplasts	**Wild type *A. thaliana*** (eco. *Col-0*)	CTP: KH9-OEP34 CPP: BP100	p*PpsbA::Rluc*	For studying the activity of spray-delivered pDNA/peptide cargos to plastids in leaf cells
Targeted gene silencing in chloroplasts	**Transplastomic *N. tabacum* line**	CTP: KH9-OEP34 CPP: BP100	*siGFPS1*	To elucidate the gene suppression function of siRNA/CTP/CPP complexes in chloroplasts

Table S10. Acquisition parameters for fluorescence imaging using confocal laser-scanned microscopy

Fluorophore	Ex/Em wavelength (nm)	Objective lens	Digital zoom	Laser power	Digital/ Fluorescence gains	Resolution (pixel^2)
TAMRA	555/580	20x/0.8 M27	2	5	1/600	512 x 512
Cy3	555/560-580	20x/0.8 M27	2	5	1/650	1024 x 1024
YFP	488/520-535	20x/0.8 M27	2	10	1/550	1024 x 1024
GFP	488/510-530	20x/0.8 M27	2	10	1/550-600[b]	1024 x 1024
Chlorophyll[a]	488/688-700	20x/0.8 M27	2	10	1/600	1024 x 1024

[a]; Chlorophyll autofluorescence in chloroplasts
[b]; Fluorescence gain = 550 for GFP fluorescence detection in chloroplasts of transplastomic tobacco leaf cells, 600 for GFP signals in GFP-overexpressing tomato leaves.

Table S11. Primers used for quantitative real-time PCR analysis

Primer name	Sequence (5’ → 3’)	Direction	Target gene
qGFP_F	CACTGCCGACAAGCAGAAGAAC	Forward	*GFP* and *YFP*
qGFP_R	CTTCTCGTTGGGGTCTTTGCTCAG	Reverse	
qAtAct2_F	TGTGCCAATCTACGAGGGTT	Forward	Arabidopsis *AtAct2*
qAtAct2_R	TTTCCCGCTCTGCTGTTGTG	Reverse	
qNtAct4_F	TGTGATGGTGGGTATGGGTC	Forward	Tobacco *NtAct4*
qNtAct4_R	GAGGCGCTTCAGTAAGGAGG	Reverse	